UNIVERSIDAD NACIONAL DE COLOMBIA

Non linear dynamics in a three cell buck converter controlled by digital PWM

Dinámica no lineal en un convertidor buck de tres celdas controlado por un PWM digital

Natalia Cañas Estrada

Universidad Nacional de Colombia
Facultad de Ingeniería y Arquitectura, Departamentode ingeniería eléctrica, electrónica y computación
Manizales, Colombia
2011

Non linear dynamics in a three cell buck converter controlled by digital PWM

Dinámica no lineal en un convertidor buck de tres celdas controlado por un PWM digital

Natalia Cañas Estrada

Thesis presented as a requirement to apply to get the master degree in:
Magister en Ingeniería - Automatización Industrial

Supervisor:
PhD. Gerard Olivar T.
Co-supervisor:
PhD. Abdelali El Aroudi.

Investigation related to:
Power electronics
Investigation group:
PCI y control inteligente

Universidad Nacional de Colombia
Facultad de Ingeniería y Arquitectura, Departamentode ingeniería eléctrica, electrónica y computación
Manizales, Colombia
2011

To my family, who supported me during this academical experience, were by my side in every single moment and trusted me in every decision I made.

”Imagination is more important than knowledge. Knowledge is limited. Imagination encircles the world.”

Albert Einstein

Acknowledgments

The pages that contain this master thesis are the fruit of two years of learning and work. Now, it is the moment to look backwards and to thank to everybody who has helped me to reach this goal. First, I want to thank my family for being supportive and standing by me all the time, for encouranging me, my crazy ideas and trusting me in every decision. I want to thank my thesis supervisor PhD. Gerard Olivar Tost for introducing me into this topic, for letting me work with him this two years and for the knowledge he shared with me. I want to specially thank my co-supervisor PhD. Abdelali El Aroudi, who showed interest in my work, invited me to go to work with him in Universitat Rovira i Virgili and who was patient enough and always supportive during the whole thesis process. Finally, I want to thank Universidad Nacional de Colombia, institution that made possible my integral enrichment through the seven years I have been studying here, for the many opportunities they gave me to acquire more knowledge such as the scholarship “Beca de estudiantes sobresalientes´´ and the economical support given to me through ”Convocatoria de apoyo a tesis´´ and ”Convocatoria de fortalecimiento de posgrados´´ to do my research stays in Universitat Rovira i Virgili in Tarragona, Spain.

I want to thank in a special way to the PCI investigation group teachers (Universidad Nacional de Colombia) and colleagues and the GAEI (Universitat Rovira i Virgili) investigation group colleagues, who were a support during the master.

Abstract

Multi-cell converters have been developed to overcome shortcomings in usual switching devices. The control systems in multi-cell converters have two main purposes: balance the voltages between the switches and regulate the load current to a desired value. In this work, a PWM digital control is applied to a three-cell buck converter. The circuit analysis was carried out by using discrete time modeling in the form of Poincaré map. Numerical simulations obtained from the mathematical model show that the system can undergo nonlinear phenomena in the form of bifurcations. This was confirmed with software to simulate circuits. Different kinds of behaviors are detected by varying some design parameters. Fixed points were found and orbital stability analysis was made. These results helped to validate bifurcation diagrams by recognizing the first bifurcation. Two and three dimensional bifurcation diagrams were also obtained. An approximation of the Poincaré map method was used as well, one and two dimensional bifurcation diagrams were obtained using it. It was also applied in the stability analysis of the fixed points.

Keywords: Discrete time model; bifurcations; multi-cell; converters; Digital PWM

Resumen

Los convertidores multicelulares se han desarrollado con el fin de mejorar las deficiencias existentes en los dispositivos de conmutación que son usados normalmente. El control en sistemas multi-celulares tiene dos propósitos principales: equilibrar las tensiones entre los switches y regular la corriente en la carga a un valor deseado. En este estudio, se utiliza un controlador digital con PWM para un convertidor buck de tres celdas.El análisis del circuito se hizo con modelado en tiempo discreto utilizando mapas de Poincaré. Se obtuvieron simulaciones numéricas usando el modelo matemático, estas muestran que el sistema puede presentar fenómenos no lineales en forma de bifurcaciones. este hecho se confirmó con un software simulador de circuitos. Varios tipos de comportamientos se pueden detectar al variar algunos parámetros de diseño. Se encontraron puntos fijos y se hizo un análisis de estabilidad de las órbitas periódicas. Estos resultados validaron los diagramas de bifurcación al detectar la primera bifurcación. Diagramas de bifurcación de dos y tres dimensional fueron obtenidos. Se utilizó también un método en el cual hay una aproximación para el método de Poincaré, de este método se obtuvieron diagramas de una y dos dimensiones. Este método también se utilizó para hacer el análisis de estabilidad de los puntos fijos.

Palabras clave: Modelado en tiempo discreto; bifurcaciones; multi-celda; convertidores; PWM Digital.

Table of Content

List of Figures

1 Introduction

Power electronics is interdisciplinary in nature and widely used in the industry. Its evolution has been incredible, the first devices which used mercury arc valves can be compared to the ones used nowadays. In the latest years, the power electronic field has been growing with the purpose of ensuring better use of existing capacity in the devices improving the efficiency. Applications in power systems often use DC-DC converters to maintain a specific voltage no matter the voltage of the battery, they are also used for electronic isolation and power factor correction.

Nowadays converters are used everywhere. Depending on the kind of converter, they can be found in different electrical devices: **AC-DC** that are used in the ones connected to the mains, change the alternating current to direct current and also voltage level if needed. The **DC-AC** converter work is to charge a DC battery when the main is available, but if the main is not working an inverter is used to produce AC electricity at mains voltage from the DC battery. **AC-AC** converters change the voltage level or frequency in alternating current and the **DC-DC** converters are used to maintain the voltage at the output, no matter the voltage of the battery, also used for electronic isolation and power factor correction.

The electronic converters need switching components to accomplish their purpose. Their presence make the system piecewise-smooth. The mathematical expressions that describe the circuit are constantly changing. The current and voltages change their values as well; as a result of this, complex dynamics like subharmonics, bifurcation and chaos are registered. Many of the studies related to power electronic DC-DC converters, specially the ones related to Buck converter, mention bifurcations and chaos, also the PWM control technique. This technique is non lineal because of the switching but is a traditional control strategy and very popular in the industry.

The system is modeled in discrete time in order to make a better study of the phenomena in the buck converter. This technique allows the reconstruction of the system behavior using Poincaré maps and also, it is used to make stability analysis of the fixed points.

The first non linear dynamic studies related to switched power electronic DC-DC converters were done by Hamill and Jeffries [1]. In this study, the operation in detail of a first order converter, bifurcation and chaotic dynamic is analyzed when controlling with PWM. Later on [2], it was studied the chaotic behavior for second order buck converters controlled by PWM.

Many researchers have contributed with their studies related to electronic power converters: A converter whose switches are changed by time-averaged models [3], The effect of the parameters in the circuit behavior analysis obtained through bifurcation diagrams and parameter mapping [4]. One-periodic and two-periodic orbits which cross the voltage ramp once per cycle and by characteristic multipliers, including as well a stability study [5]. Second order DC-DC Boost converter under current programmed control with and without voltage feedback [6]. The study field started growing with even more contributions such as the possibility of using local transversal Lyapunov exponents for characterization of chaotic systems synchronization [7].

The most important contribution to this area was Di Bernardo's work [8] [9], in which proposes and proves a new discrete application for bifurcation and chaos analysis in DC-DC converters controlled by PWM. Other studies that complement and have been developed, are related to border collision bifurcations for a current feedback-controlled buck converter [10], Charactersitic multipliers of a periodic orbit computed analytically to obtain the values for smooth and non-smooth bifurcations [11], two-parameter bifurcation diagrams acquired through computer simulations in which the results obtained with the simulation were compared to the ones that were obtained with the physical model [12].

Due to this mentioned studies, this research field is continuosly changing and getting wider. Many contributions give continuity to the related topics and research lines included in the power electronic field. There are international articles, theses and many other researches that show how the theory has evolved. The Fixed-frequency quasi-sliding control algorithm based on switching surface zero averaged dynamics (ZAD), was applied to the design of a Buck-based inverter and was implemented in a laboratory prototype by means of a field programmable gate array (FPGA), in [13]. A study by Angulo [14], used FPIC and ZAD techniques as chaos transition based on the Poincaré application, and control design for chaotic operation was compared to TDAS technique, gave as a result a shorter circuit response and lower error signal. Also, the experimental results proved non-linear phenomena and stability limits. Another studies contributed to other parts of the field, Switched systems theory was deeply studied and it is registered in [15], Non linear dynamic analysis in multi-cell converters became a topic of interest [16].

Numerous studies related to multi-cell converters have been done. These helped understand the new converters configuration behavior. One of the first studies was developed by Gateau et al. [17]. Here, there are exposed different approaches to represent these systems mathematically. The techniques are compared and to conclude the study, it was stated the average value model was the most optimal choice because it allows to obtain, in a very accurate way, the system dynamic behavior. This technique also allows to make the analysis as good and efficient as possible, through studying the stability of limit cycles with discrete time modeling.

Some other reported studies are related to the use of discrete time modeling for multi-cell DC-DC

converters [18], the dynamics and stability analysis for the two-cell Buck converter for high and medium voltage applications [19], the use of FPIC control to widen the stability zone in two-cell buck converters [20] and to stabilize it [21]. And alternative control methods for four-level three-cell DC-DC buck converter [22].

In order to study these circuits behavior, it is important to understand the non linear dynamics that are registered in non linear systems; even when the reported studies include an explanation of the dynamics on the treated converter configuration, there are some studies [23] [24] that help understand the phenomenon and explain the terminology used in the analysis.

The content of this thesis is related to the three-cell buck converter controlled by a digital PWM. The main objective is to analyze the dynamic behavior of this specific converter by using accurate mathematical simulation and an appropriate modeling of the observed phenomena. The control is done using digital PWM, which is a contribution to the research field. This is a non-studied way to control this specific converter configuration. It is exposed, explained and analyzed. This analysis includes: develop and evaluation of the mathematical state space, analysis of the effect of the system parameters, one and two dimensional bifurcation diagrams validation, the obtaining of fixed points and conclusions related to stability analysis and comparing results with the system simulation.

Being a mathematical process, it is important to have an efficient algorithm. The implemented algorithm allows to obtain results without waiting too much. The usage of the discrete time modeling as circuit reconstruction method and by taking advantage of the digital control, the general process to describe the system is simple and accurate. The poincaré maps of periodic orbits are also studied, including stability analysis.

Chapter two contains the system explanation in general, how it works, the different configurations that the circuit can take, the possible switches state and how to obtain the equations that rule variables behavior. Chapter three contains the explanation related to the used control technique, the saturation function and the discrete time modeling implemented in the algorithm. Chapter four contains the state space analysis: a reference circuit is taken, the results obtained with this parameter configuration are compared to the results obtained for the system with different parameter values; the inductor, capacitors and resistance values are changed and the analysis of the circuit response is carried out for different current feedback coefficients. In chapter five, the obtained bifurcation diagrams are analyzed in order to observe and come up with a conclusion related to the circuit behavior when using certain parameter values, as well as an analysis of the nonlinear dynamics presented. Chapter six, exposes two parameter bifurcations which allow to make a deeper analysis of the periodicity per parameters combination.

All the algorithm results are compared to simulations made with PSIM software. All proves and

simulations were made with values that power electronic converters take when they are implemented in practice.

2 System description

2.1 Three-cell DC-DC buck converter

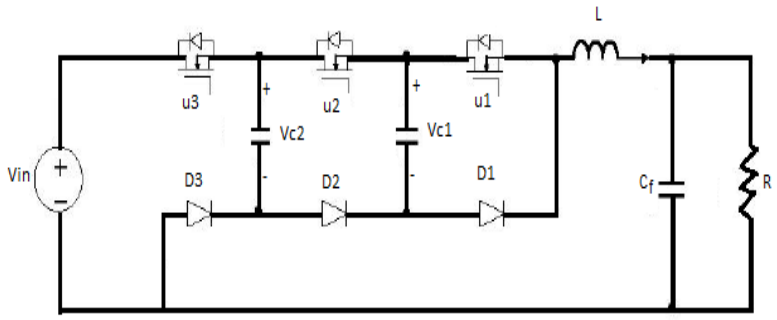

Figure 2-1: Three-cell buck converter with a capacitor in parallel with the load

Let us consider the three-cell DC-DC buck converter in figure 2.1. This circuit works with three branches formed by a switch u_i and the respective diode D_i, where index i is used to differentiate the three cells with each other ($i = 1, 2, 3$). They are enumerated from right to left. The three cell buck converter also has an inductor L and a constant input voltage V_{in}.

When u_i is **ON**, D_i must be **OFF** and vice versa; this means, that the circuit changes its structure when some conditions on the state variables or time happen. Its behavior is described by eight different systems. Each cell is controlled by an output signal s_i; when s_i is equal to 1 **(ON)**, the switch is conducting and the diode D_i blocks the current and when s_i is equal to 0 **(OFF)**, which means that the switch acts like an open circuit but the diode D_i lets the current flow.

The circuit in the figure 2.1 has a flying capacitor C_f in parallel to the resistor. This capacitor prevents the ripple of the output voltage from being big. Because of this, the output voltage can be considered constant. In the mathematical analysis, the three-cell DC-DC buck converter can be considered without this filtering capacitor in parallel with the load (see fig. 2.1), because it is not necessary. It is enough to control the inductor current, the output voltage can be controlled with the current control and measured in the load. The switching process is done using feedback coefficients [21].

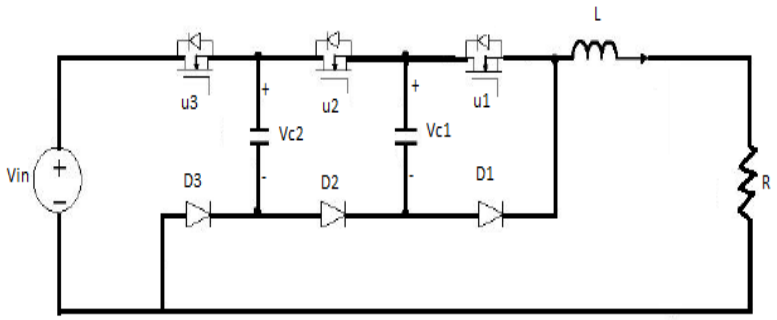

Figure 2-2: Three-cell buck conventer used for the study

All the linear time invariant equations are given in the form $\dot{x} = A_k x + B_k$. x is the vector of state variables, A_k is the system matrix and B_k is the input vector. The components of these matrices and vectors are R, L, C_1, C_2 and V_{IN}, which are the system parameters and k defines the active configuration $(k = 1, 2, ..., M)$, where M is the total number of configurations per period.

The system and input matrices for each configuration are obtained using kirchhoff laws:

- **Configuration 1 (ON,ON,ON)**
  In this configuration, the inductor L is charged and the charges in C_1 and C_2 are maintained.

$$A_1 = \begin{bmatrix} \frac{-R}{L} & 0 & 0 \\ 0 & 0 & 0 \\ 0 & 0 & 0 \end{bmatrix} \quad ; \quad B_1 = \begin{bmatrix} \frac{Vin}{L} \\ 0 \\ 0 \end{bmatrix}$$

- **Configuration 2 (ON,ON,OFF)**
  During this configuration, L is charged, C_1 charge is maintained and C_2 is discharged.

$$A_2 = \begin{bmatrix} \frac{-R}{L} & 0 & \frac{1}{L} \\ 0 & 0 & 0 \\ \frac{-1}{C_2} & 0 & 0 \end{bmatrix} \quad ; \quad B_2 = \begin{bmatrix} 0 \\ 0 \\ 0 \end{bmatrix}$$

- **Configuration 3 (ON,OFF,OFF)**
  The inductor L is discharged, C_1 is discharged and C_2 charge is maintained.

$$A_3 = \begin{bmatrix} \frac{-R}{L} & \frac{1}{L} & 0 \\ \frac{-1}{C_1} & 0 & 0 \\ 0 & 0 & 0 \end{bmatrix} \quad ; \quad B_3 = \begin{bmatrix} 0 \\ 0 \\ 0 \end{bmatrix}$$

- **Configuration 4 (OFF,OFF,OFF)**
  During this configuration, L is discharged, the capacitors C_1 and C_2 charge is maintained.

$$A_4 = \begin{bmatrix} \frac{-R}{L} & 0 & 0 \\ 0 & 0 & 0 \\ 0 & 0 & 0 \end{bmatrix} \quad ; \quad B_4 = \begin{bmatrix} 0 \\ 0 \\ 0 \end{bmatrix}$$

- **Configuration 5 (OFF,ON,ON)**
  During this configuration, L is charged, C_1 charge is charged and C_2 charge is maintained.

$$A_5 = \begin{bmatrix} \frac{-R}{L} & \frac{-1}{L} & 0 \\ \frac{1}{C_1} & 0 & 0 \\ 0 & 0 & 0 \end{bmatrix} \quad ; \quad B_5 = \begin{bmatrix} \frac{Vin}{L} \\ 0 \\ 0 \end{bmatrix}$$

- **Configuration 6 (OFF,OFF,ON)**
  During this configuration, L is discharged, C_1 charge is maintained and C_2 is charged.

$$A_6 = \begin{bmatrix} \frac{-R}{L} & 0 & \frac{-1}{L} \\ 0 & 0 & 0 \\ \frac{1}{C_2} & 0 & 0 \end{bmatrix} \quad ; \quad B_6 = \begin{bmatrix} \frac{Vin}{L} \\ 0 \\ 0 \end{bmatrix}$$

- **Configuration 7 (OFF,ON,OFF)**
  During this configuration, L is discharged, C_1 is charged and C_2 is discharged.

$$A_7 = \begin{bmatrix} \frac{-R}{L} & \frac{-1}{L} & \frac{1}{L} \\ \frac{1}{C_1} & 0 & 0 \\ \frac{-1}{C_2} & 0 & 0 \end{bmatrix} \quad ; \quad B_7 = \begin{bmatrix} 0 \\ 0 \\ 0 \end{bmatrix}$$

- **Configuration 8 (ON,OFF,ON)**
  During this configuration, L is charged, C_1 is discharge and C_2 is charged.

$$A_8 = \begin{bmatrix} \frac{-R}{L} & \frac{1}{L} & \frac{-1}{L} \\ \frac{-1}{C_1} & 0 & 0 \\ \frac{1}{C_2} & 0 & 0 \end{bmatrix} \quad ; \quad B_8 = \begin{bmatrix} \frac{Vin}{L} \\ 0 \\ 0 \end{bmatrix}$$

To obtain an accurate study of the three-cell DC-DC buck converter, a systematic nonlinear discrete time model is presented. The main objective is to observe the complex behavior that this system can have. This model will have the general matrices A and B given by:

$$A = \begin{bmatrix} \frac{-R}{L} & \frac{-1}{L}(u_2 - u_1) & \frac{-1}{L}(u_3 - u_2) \\ \frac{1}{C_1}(u_2 - u_1) & 0 & 0 \\ \frac{1}{C_2}(u_3 - u_2) & 0 & 0 \end{bmatrix} \quad ; \quad B = \begin{bmatrix} \frac{V_{in}}{L} u_3 \\ 0 \\ 0 \end{bmatrix} \tag{2-1}$$

where u_i is the binary command signal for the switches u_i and they are given by:

$$u_i = \begin{cases} 1 & if \;\; s_i \;\; is \;\; closed \;\; (ON) \\ 0 & if \;\; s_i \;\; is \;\; open \;\; (OFF) \end{cases} \tag{2-2}$$

The main advantage of this structure is the fact that the floating capacitors allow to distribute the voltage across the blocking switches. The voltage in any blocking switch u_i is given by the difference between the capacitors C_i y C_{i-1}, and this value is known as the cell voltage. The specified cell is know by the suffix $_i$ [16].

2.2 Digital PWM control

This buck converter configuration has three cells which are controlled by three PWM signals. These signals have to be phase shifted $2\pi/3$ between each other. The phase shift can be chosen freely, but if they are phase shifted 2π/p, where **p** is the total number of cells, it is possible to cancel harmonics that might appear [25].

The control objective is to drive the system to a periodic orbit with a fixed frequency in steady state, with a desired average value for the state variables. In this multi-cell converters without flying capacitor in paralell to the load, the purpose is to control the inductor current with the purpose to make it achieve the value given by the reference signal I_{ref}. The voltage in capacitor C_1 must be $1/3$ of the input voltage V_{IN} and the voltage in capacitor C_2 must be $2/3$ of the same input voltage V_{IN}. This technique will allow to reduce the stress in the switches and to obtain voltage balance and duty cycles as similar as it is possible.

Digital control is used for this study because of the advantages it has. Just to name some of them: insensitivity to noise and programmability [26]. In order to describe the converter behavior, an algorithm is created using the mathematical equations that describe the circuit. The non linear system is obtained using discrete time modeling. This model takes into account the natural saturations of the PWM duty cycle, this explanation is detailed after the control signals explanation.

There are many strategies to control the system. The one used in this study, is based on proportional feedback control. In the control signals, there are three different feedback coefficients k_i, k_{v_1} and k_{v_3}. One feedback coefficient for each variable, which multiply their respective variable error signal. The control signals s_i that are:

$$\begin{aligned} s_1 &= k_i(i_{REF} - i_L) - k_{v1}(\tfrac{1}{3}V_{IN} - V_{C_1}) \\ s_2 &= k_i(i_{REF} - i_L) \\ s_3 &= k_i(i_{REF} - i_L) - k_{v3}(\tfrac{2}{3}V_{IN} - V_{C_2}) \end{aligned} \tag{2-3}$$

For these signals, the current in the inductor and voltages in capacitors are sampled through time when each period starts. This value is saved and compared to the reference value given for the corresponding variable. The error signal is obtained. This control receives the name of **Digital PWM control** due to the use of digital "sample and hold" structures to maintain the control signal values until the end of the period.

Each control signal s_i is compared to a PWM or sawtooth function. In total, there are three sawtooth functions. Each one is phase shifted $2\pi/3$ with respect to each other, where 3 is the number

of cells. This settled phase shift helps to prevent the appearance of harmonics.

The sawtooth functions are given by:

$$\begin{aligned} h_1(t) &= (V_u - V_l)\tfrac{t}{T} \mod 1 \\ h_2(t) &= (V_u - V_l)\tfrac{t-\frac{T}{3}}{T} \mod 1 \\ h_3(t) &= (V_u - V_l)\tfrac{t-\frac{2T}{3}}{T} \mod 1 \end{aligned} \tag{2-4}$$

where V_u and V_l are the upper and lower values that the sawtooth functions take. In this case, V_u = 1 V and V_l = 0 V. **t** is the exact moment of time in which the signal is sampled and **T** is the period of the sawtooth.
The control works this way: if s_k is greater than h_k, then the switch is **ON** and vice versa.

The duty cycles are directly proportional and equal to the control signal s_i values. To be more specific, it depends if they are bigger or lower than the corresponding PWM. The sawtooth functions amplitude is 1 V, being upper value is 1 V. The duty cycle coincides with the value of the correspondent control signal at the beginning of each period. The bigger the value the control signal registers, the bigger the duty cycle that corresponds to that control signal is.

$$d_i = s_i \tag{2-5}$$

If the control signal s_i takes a value between 0 and 1, the duty cycle for that period will take the same value. But if the control signal value is equal or higher than 1, or if it is lower or equal to 0, there will not be a change in the state of the corresponding switch in that period, and a saturation function is applied to narrow the duty cycles. A new d_i function is given by:

$$d_i = sat(s_i) = \frac{1}{2}(1 + |s_i| - |s_i - 1|) \tag{2-6}$$

The duty cycles expressions are given by:

$$\begin{aligned} d_1 &= \text{sat}\left[k_i(I_{ref} - x_1) - k_{v1}(\tfrac{1}{3}V_{in} - x_2)\right] \\ d_2 &= \text{sat}\left[k_i(I_{ref} - x_1)\right] \\ d_3 &= \text{sat}\left[k_i(I_{ref} - x_1) + k_{v3}(\tfrac{2}{3}V_{in} - x_3)\right] \end{aligned} \tag{2-7}$$

Every time there is a switch in one of the semiconductors, the circuit changes its configuration and also the equations that describe the system change.

This saturation signals are applied to the general matrices A and B (3-2), which used to have the switches positions instead of the duty cycles. The new matrices are given by:

$$A = \begin{bmatrix} \frac{-R}{L} & \frac{-1}{L}(d_2 - d_1) & \frac{-1}{L}(d_3 - d_2) \\ \frac{1}{C_1}(d_2 - d_1) & 0 & 0 \\ \frac{1}{C_2}(d_3 - d_2) & 0 & 0 \end{bmatrix} \quad ; \quad B = \begin{bmatrix} \frac{V_{in}}{L}d_3 \\ 0 \\ 0 \end{bmatrix} \tag{2-8}$$

3 Mathematical modeling

3.1 Discrete time modeling - Open loop

Discontinuous Piecewise Affine (DPWA) periodically driven systems is a term introduced by El Aroudi et al. [27]. The three cell buck converter is a DPWA system characterized by a finite number of affine dynamical models together with some switching conditions to change from one model to another. As a result, there is a state of space partitioning into different cells which are described by a different affine equation. When the switch action changes the system configuration due to the discontinuity of the vector field, smoothness is lost when the boundary is crossed; this event is called **non smoothness sets** or **switching manifolds** [27].

To obtain the matrices A_1 and B_1 at the start moment $t = 0$, the initial values of the switches u_i are replaced in the general A and B matrices in eq. (2-8). These values depend on the initial conditions of the variables, see eq. (2-2). Once the matrices are obtained, the given initial conditions have to be organized in a vector x_0 and must be replaced in x. The procedure consists on solving an arrange of ordinary differential equations with a given initial point. The equation (3-1) is used to describe the system.

$$\dot{x} = A_k x + B_k \tag{3-1}$$

where $x \in R^N$, is the vector of state variables and N represent the amount of variables to control, for this case, $N = 3$. $A_k \in R^{N \times N}$ and $B_k \in R^{N \times 1}$ are the system matrices and vectors during each phase. Each phase is determined by the switching action and the components are the system parameters. k takes values between 1 to 6, the length of k depends on the switches saturation (if they are saturated $k < 6$, if they are not saturated $k = 6$) and it indicates the maximum number of configurations per period. The matrices A and B depend on the switches u_i state between $nT + t_{k-1}$ and $nT + t_k$. The systems can be described by these equations:

$$\begin{array}{lll}
\dot{x} = A_1 x + B_1 & for & nT \leq t < nT + t_1 \\
\dot{x} = A_2 x + B_2 & for & nT + t_1 \leq t < nT + t_2 \\
\dot{x} = A_3 x + B_3 & for & nT + t_2 \leq t < nT + t_3 \\
\dot{x} = A_4 x + B_4 & for & nT + t_3 \leq t < nT + t_4 \\
\dot{x} = A_5 x + B_5 & for & nT + t_4 \leq t < nT + t_5 \\
\dot{x} = A_5 x + B_6 & for & nT + t_5 \leq t < (n+1)T
\end{array} \tag{3-2}$$

During each subinterval, the equations are time invariant and the solution can be obtained by [27]:

$$x(t) = e^{A_k(t-t_0)} x_0 + \int_{t_0}^{t} e^{A_k \alpha} B_k d\alpha \tag{3-3}$$

where t_o is the initial time [28].

The mapping that makes the relation between the state variables x_n at the beginning of an entire cycle and x_{n+1}, is based on stroboscopic sampling at the beginning of each period. The following expression is obtained:

$$x_{n+1} = P(x_n) \tag{3-4}$$

3.1.1 The open loop discrete time model in the Three-cell buck converter

In this study, the values taken for the parameters are given by: $V_{in} = 1200\,V$, capacitance $C_1 = 22\,\mu F$, capacitance $C_2 = 22\,\mu F$, inductance $L = 1\,mH$, load resistance $R = 10\,\Omega$, switching period selected is $T = 25\,\mu s$. The lower and upper voltages of the repetitive saw-tooth signals are $V_l = 0\,V$ and $V_u = 1\,V$. The feedback coefficients are taken as follows $k_{v1} = k_{v3} = 0.01$ and $k_i = 0.05$.

For these values, once the circuit response stabilizes, the circuit duty cycles obtaineded are between 33 % and 66 % . Following this logic, as the duty cycle depends on the control signals, it means that they take values between 0.33 V and 0.66 V. This hypothesis can be confirmed with the figures shown in chapter 4.

The pattern of the configuration that rules each period lies on the duty cycles. This particularity is presented because of the digital PWM control, which by maintains the first value each variable take per period until the end of it. The system variables change their values as time goes on, but these new values are neglected for the control signals but they are taken into account when a switching actions occurs and a as a result, there is a configuration change. Each time there is a new configuration, the last value the system variables took, is taken as initial condition for the same variable in the new configuration analysis. For these parameter values, the next pattern appears in the steady state.

$$C_{onf_8} \rightarrow C_{onf_3} \rightarrow C_{onf_2} \rightarrow C_{onf_7} \rightarrow C_{onf_5} \rightarrow C_{onf_6}$$

For this pattern, the switched model that describes the three-cell buck converter is:

$$\begin{aligned}
\dot{x} &= A_8 x + B_8 \quad for \quad nT \leq t \leq nT + t_1 \\
\dot{x} &= A_3 x + B_3 \quad for \quad nT + t_1 \leq t \leq nT + t_2 \\
\dot{x} &= A_2 x + B_2 \quad for \quad nT + t_2 \leq t \leq nT + t_3 \\
\dot{x} &= A_7 x + B_7 \quad for \quad nT + t_3 \leq t \leq nT + t_4 \\
\dot{x} &= A_5 x + B_5 \quad for \quad nT + t_4 \leq t \leq nT + t_5 \\
\dot{x} &= A_6 x + B_6 \quad for \quad nT + t_5 \leq t \leq (n+1)T
\end{aligned}$$

where the corresponding A and B matrices are given by the same ones in section 2.1.

These configurations are by using eq. (3-3). The variable values are obtained and taken as the initial values for the following equation.

3.2 Discrete time modeling - Closed loop

3.2.1 Simplified dimensionless discrete time model

Let $i_{L,k}$ be the inductor current, $V_{C1,k}$ and $V_{C2,k}$ be the voltage in capacitor 1 and the voltage in capacitor 2 respectively at time instant kT. If rectilinear waveforms are assumed for the state variables, the following approximate model is obtained:

$$\begin{bmatrix} i_{L,k+1} \\ V_{C1,k+1} \\ V_{C2,k+1} \end{bmatrix} = \begin{bmatrix} 1-\frac{RT}{L} & \frac{-T}{L}(d_2-d_1) & \frac{-T}{L}(d_3-d_2) \\ \frac{T}{C_1}(d_2-d_1) & 1 & 0 \\ \frac{T}{C_2}(d_2-d_1) & 0 & 1 \end{bmatrix} \begin{bmatrix} i_{L,k} \\ V_{C1,k} \\ V_{C2,k} \end{bmatrix} + \begin{bmatrix} \frac{V_{IN}T}{L}d_3 \\ 0 \\ 0 \end{bmatrix} \quad (3\text{-}5)$$

In practical DC-DC power electronics converters, it is always true that the switching period is smaller than the time constants of the circuit in such a way that the matrix exponential e^{At} can be linearized [28]. It has been shown in [18] [28] that $e^{At} \approx I + At$ can be used to obtain PWL trajectories [21]. Using this approximation and neglecting second and higher terms, it is possible to obtain the simple approximated model in equation (3-5).mThis approximation helps to improve the computational time spent for calculations, which is an improvement if the idea is to make more complex analysis such as bifurcation diagrams.

In order to simplify the model, dimensionless variables and parameters are considered: the current is scaled by the maximum current available in the circuit (given by $I_{max} = V_{in}/R$) and the voltages are scaled to the maximum voltage in the circuit which is the input voltage V_{in}. Time is normalized by the switching period T, which is the same of the PWM.

The changes for the variables and parameters are given by the following mathematical relations:

$$Parameters \quad \rightarrow \quad \delta_L = \frac{RT}{L}\ ; \qquad \delta_{C1} = \frac{T}{RC_1}\ ; \qquad \delta_{C2} = \frac{T}{RC_2} \quad (3\text{-}6)$$

$$Variables \quad \rightarrow \quad x_{1,k} = \frac{Ri_{L,k}}{V_{IN}}\ ; \qquad x_{2,k} = \frac{V_{C1}}{V_{IN}}\ ; \qquad x_{3,k} = \frac{V_{C2}}{V_{IN}} \quad (3\text{-}7)$$

After this changes take place, the following dimensionless model is obtained:

$$\begin{bmatrix} x_{1(n+1)} \\ x_{2(n+1)} \\ x_{3(n+1)} \end{bmatrix} = \begin{bmatrix} 1-\delta_L & -\delta_L(d_2-d_1) & -\delta_L(d_3-d_2) \\ \delta_{C1}(d_2-d_1) & 1 & 0 \\ \delta_{C2}(d_2-d_1) & 0 & 1 \end{bmatrix} \begin{bmatrix} x_{1,k} \\ x_{2,k} \\ x_{3,k} \end{bmatrix} + \begin{bmatrix} \delta_L d_3 \\ 0 \\ 0 \end{bmatrix} \tag{3-8}$$

Reducing the ripple through the load and the voltage ripple across the capacitor would improve the results. The ripple is reduced when the circuit parameters are able to satisfy $\delta_L << 1$, $\delta_{C1} << 1$ and $\delta_{C2} << 1$. The system new dimensionless variables are $x_{1,k} = Ri_{L,k}/V_{IN}$, $x_{2,k} = V_{C2,k}/V_{IN}$ and $x_{3,k} = V_{C3,k}/V_{IN}$. For the values taken the new dimensionless parameters values are:

$$\delta_L = 0.25 \ ; \qquad \delta_{C1} = \delta_{C2} = 0.1136 \tag{3-9}$$

The expression of the dimensionless duty cycles in the kth cycle is given by:

$$\begin{aligned} d_{1,k} &= \text{sat}\left[k_1(I_R - x_{1,k}) - k_2(\tfrac{1}{3} - x_{2,k})\right] \\ d_{2,k} &= \text{sat}\left[k_1(I_R - x_{1,k})\right] \\ d_{3,k} &= \text{sat}\left[k_1(I_R - x_{1,k}) + k_3(\tfrac{2}{3} - x_{3,k})\right] \end{aligned} \tag{3-10}$$

Where $I_R = I_{ref}(R/V_{IN})$, $k_1 = k_i(V_{IN}/R)$, $k_2 = k_{V1}V_{IN}$ and $k_3 = k_{v3}V_{IN}$. In a matrix form, these duty cycles can be written as:

$$d_{i,k} = \begin{bmatrix} d_{1,k} \\ d_{2,k} \\ d_{3,k} \end{bmatrix} = sat \begin{bmatrix} k_1 & -k_2 & 0 \\ k_1 & 0 & 0 \\ k_1 & 0 & k_3 \end{bmatrix} \begin{bmatrix} I_R - x_{1,k} \\ \frac{1}{3} - x_{2,k} \\ \frac{2}{3} - x_{3,k} \end{bmatrix} \tag{3-11}$$

Now, to obtain the closed-loop non-linear map that describes the three-cell buck converter, eq. (3-11) must be substituted in eq. (3-8). Notice that this model is only linear when d_1, d_2 and d_3 are saturated. Due to this saturation, the closed-loop function is piecewise smooth and is described

by the next equation array:

$$x_{k+1} = \begin{cases} A_1 x_k + B_1 & \text{if} \quad F_1(x_{2,k}) > x_{1,k} \\ A_d x_k + B_d & \text{if} \quad F_1(x_{2,k}) < x_{1,k} < F_0(x_{2,k}) \\ A_0 x_k & \text{if} \quad F_0(x_{2,k}) < x_{1,k} \end{cases} \tag{3-12}$$

where

$$\begin{aligned} A_d &= \begin{bmatrix} 1-\delta_L & -\delta_L(du_{2,k}-du_{1,k}) & -\delta_L(du_{3,k}-du_{2,k}) \\ \delta_{C1}(du_{2,k}-du_{1,k}) & 1 & 0 \\ \delta_{C2}(du_{2,k}-du_{1,k}) & 0 & 1 \end{bmatrix} \\ A_1 &= \begin{bmatrix} 1-\delta_L & 0 & 0 \\ 0 & 1 & 0 \\ 0 & 0 & 1 \end{bmatrix} \qquad B_1 = \begin{bmatrix} \delta_L \\ 0 \\ 0 \end{bmatrix} \\ B_d &= \begin{bmatrix} \delta_L du_{3,k} \\ 0 \\ 0 \end{bmatrix} \qquad A_0 = A_1 \end{aligned} \tag{3-13}$$

And the reference limits are given by:

$$\begin{aligned} F_1(x_{2,k}) &= I_R + \tfrac{k_3}{k_1}\left(\tfrac{2}{3} - x_{3,k}\right) \\ F_0(x_{2,k}) &= I_R - \tfrac{k_2}{k_1}\left(\tfrac{1}{3} - x_{2,k}\right) \end{aligned} \tag{3-14}$$

3.3 Poincaré maps

3.3.1 Existence conditions of periodic orbits

In a system with M different configurations, there are different types of periodic orbits, but only one of them is desired from a practical point of view. The most interesting periodic orbit in an engineering point of view, is the one that happens after the switching through the M configurations

per cycle [27].

Definition. A periodic orbit that is characterized by M and only M different configurations during one switching cycle is called **M-modal periodic orbit**. A M-modal periodic orbit $x^*(t)$ will exist if there exists a vector $(t_1, t_2, ..., t_{M-1})$ such that the following conditions hold [27]:

1. $x^*(kT) = x^*((k+1)T) \forall k = 1, ..., M$
2. $\dot{x}^*(t) = A_k x^*(t) + B_k$ for $t \in (t_{k-1}, t_k) \forall k = 1, ..., M$.

When the system has a stable behavior, there are periodic orbits that satisfy these conditions.

3.3.2 Poincaré map of periodic orbits

As mentioned in a prior study by El Aroudi et al. [16], the usefulness of the poincaré map **P** results from the fact that its fixed points X^* correspond to periodic orbits x^* of the continuous time switched system and that the stability properties are the same for both of them. The piecewise affine character of the system allows to obtain the fixed points of **P** in terms of time instants t_k [27] [16].

$$\varphi_k(t, x_{k-1}) = \phi_k(t) x_{k-1} + \psi(t) B_k \tag{3-15}$$

where:

$$\phi_k(t) = e^{At} \tag{3-16}$$

The expression for $\psi(t)$ depends on the characteristics of the A matrix. If A matrix is invertible, $\psi(t)$ is given by :

$$\psi(t) = A^{-1}(\phi_k(t) - 1) \tag{3-17}$$

and in general, $\psi(t)$ is given by the following expression:

$$\psi(t) = \int_0^t e^{A\alpha} d\alpha \tag{3-18}$$

Where $\mathbf{1}$ is the identity matrix with appropriate dimension. If A is singular, using time series expansion the next expression is obtained:

$$\psi(t) = (\mathbf{1}t + \frac{At^2}{2} + \frac{A^2t^3}{6} + ... + \frac{A^k t^{k+1}}{(k+1)!} + ...) \tag{3-19}$$

In the three-cell buck converter, the A matrices for all configurations are singular, which means the equation (3-17) can not be used. In order to describe the system behavior from the beginning of the period until the end of it, it is necessary to use the poincaré map expression. The expression for P can be written as [27]:

$$P(x_n, t) = \phi(t)x_n + \psi(t) \tag{3-20}$$

where t is a column vector that has the time durations for each configuration and $\phi(t)$ is defined by:

$$\phi(t) = \prod_{k=M}^{1} \phi_k(t_k) \tag{3-21}$$

For the three-cell buck converter, $\phi(t)$ is given by the following expression:

$$\phi(t) = e^{A_6(t_6-t_5)} e^{A_5(t_5-t_4)} e^{A_7(t_4-t_3)} e^{A_2(t_3-t_2)} e^{A_3(t_2-t_1)} e^{A_8 t_1} \tag{3-22}$$

where the matrices A_{conf} and B_{conf} are the ones in section 2.1, which depend on the configuration active in the moment of the analysis. $t_1, t_2, t_3, t_4, t_5, t_6$ are part of the switching moments vector given by τ. This vector depends on the duty cycles of the switches. When the system operates in closed loop, the τ vector indicates when there is a crossing between the ramp and the respective control signal. For open loop, this switching instants are previously given [27].

The general expression for $\psi(\tau)$ is given by:

$$\psi(t) = \sum_{j=1}^{M-1} \prod_{k=M}^{j+1} \phi_k(t_k)\psi_j(t_j)B_j + \psi_M(t_M)B_M \tag{3-23}$$

for the three-cell buck converter, the $\psi(t)$ expression is

$$\begin{aligned}
\psi(t) &= e^{A_6(t_6-t_5)}e^{A_5(t_5-t_4)}e^{A_7(t_4-t_3)}e^{A_2(t_3-t_2)}e^{A_3(t_2-t_1)}\int_0^{t_1} e^{A_8\alpha}B_8 d\alpha + \dots \\
&\dots + e^{A_6(t_6-t_5)}e^{A_5(t_5-t_4)}e^{A_7(t_4-t_3)}e^{A_2(t_3-t_2)}\int_{t_1}^{t_2} e^{A_3\alpha}B_3 d\alpha + \dots \\
&\dots + e^{A_6(t_6-t_5)}e^{A_5(t_5-t_4)}e^{A_7(t_4-t_3)}\int_{t_2}^{t_3} e^{A_2\alpha}B_2 d\alpha + \dots \\
&\dots + e^{A_6(t_6-t_5)}e^{A_5(t_5-t_4)}\int_{t_3}^{t_4} e^{A_7\alpha}B_7 d\alpha + e^{A_6(t_6-t_5)}\int_{t_4}^{t_5} e^{A_5\alpha}B_5 d\alpha + \int_{t_5}^{t_6} e^{A_6\alpha}B_6 d\alpha
\end{aligned} \tag{3-24}$$

3.3.3 Poincaré map of the open-loop and closed-loop system

As mentioned before, in open loop systems, the switching instants are already known, they are given a priori because of the duty cycle. The change of configurations appears in a fixed pattern each period once the circuit stabilizes. Eq. (3-1) can also be expressed as follows:

$$x(t) = \varphi_k(t, x_0) \tag{3-25}$$

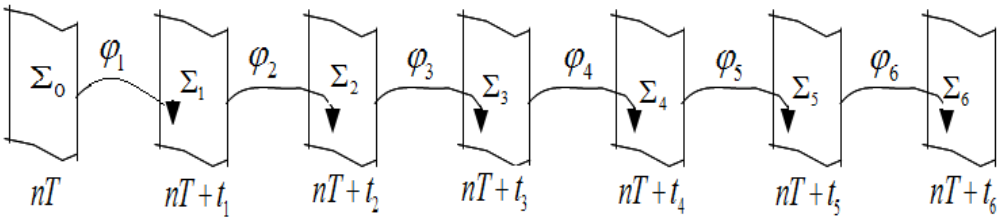

Figure 3-1: Partitioning of the state space into different cells

where x_0 is an arbitrary initial condition.

If the system changes its structure from configuration C_{onf_k} to configuration $C_{onf_{k+1}}$, there is also a change in the function that describes it. The trajectory between these two functions is given by φ_k. It starts with the initial condition x_{k-1} on a surface $\sum_{k-1}$, this surface reaches $\sum_k$ at time moment t_k measured by the difference between the $k_{th}-1$ cycle until k-th cycle. The manifold to come depends on the actual one and all the variables values defined by the exact moment when the switching action takes place. In other words, $\sum_k$ are switching manifolds given by fixed switching moments. Each switching cycle, the local maps P_k are obtained this way:

$$
\begin{aligned}
&P_1 : \Sigma_0 \to \Sigma_1 \\
&x_n \to x(t_1) := \varphi_1(t_1, x_n) \\
&P_2 : \Sigma_1 \to \Sigma_2 \\
&x(t_1) \to x(t_2) := \varphi_2(t_2 - t_1, x(t_1)) \\
&P_3 : \Sigma_2 \to \Sigma_3 \\
&x(t_2) \to x(t_3) := \varphi_3(t_3 - t_2, x(t_2)) \\
&\vdots \\
&P_M : \Sigma_{M-1} \to \Sigma_M \\
&x(t_{M-1}) \to x_{n+1} := \varphi_M(T - t_{M-1}, x(t_{M-1}))
\end{aligned}
\tag{3-26}
$$

where $t_k (k = 1, 2, ..., M-1)$ is a vector of configuration switching moments in time. The poincaré map from $\sum_0$ to $\sum_0$ is defined by the composition of the M different local mapping P_k:

$$
\begin{aligned}
&P : \Sigma_0 \to \Sigma_0 \\
&P : P_M \circ P_{M-1} \circ \cdots P_1
\end{aligned}
\tag{3-27}
$$

$$x_n \to x_{n+1} := P(\tau, x_n) = \varphi_M(T - t_{M-1}, \varphi_{M-1}(t_{M-1} - t_{M-2}, \varphi_{M-2}(\cdots))) \tag{3-28}$$

$$\begin{aligned} &P : x_n \to x_{n+1} \\ &P : e^{A_6(t_6-t_5)}(e^{A_5(t_5-t_4)}(e^{A_7(t_4-t_3)}(e^{A_2(t_3-t_2)}(e^{A_3(t_2-t_1)}(e^{A_8 t_1}x_o + \int_0^{t_1} e^{A_8\alpha}B_8 d\alpha) + \cdots \\ &\cdots + \int_{t_1}^{t_2} e^{A_3\alpha}B_3 d\alpha) + \int_{t_2}^{t_3} e^{A_2\alpha}B_2 d\alpha) + \int_{t_3}^{t_4} e^{A_7\alpha}B_7 d\alpha) + \int_{t_4}^{t_5} e^{A_5\alpha}B_5 d\alpha) + \int_{t_5}^{t_6} e^{A_6\alpha}B_6 d\alpha \end{aligned} \tag{3-29}$$

where $\tau = t_k = (t_1, t_2, ..., t_{M-1})^t$ is the configuration switching moments vector. In this analysis, it is considered that the switching is due to the existence of a T-periodic function, so for open loop systems, there can be only nominal periodic orbits with period T. Equilibrium points are possible, only in case the system remains blocked in some configuration and no switching involved [27].

The interest now is centered then in M-modal periodic orbits. If this kind of orbits exist in the circuit, the fixed time durations have to be already known, so the associated periodic orbit can be computed. In order to find the time durations, it is necessary to solve a set of transcendental equations that compare the repetitive sawtooth function and the control signals.

The stability for this case is a local issue, but in open-loop stability is global. If the switching function σ_k defining the switching manifolds $\sum_k$ can be written as the difference between a state dependent function $s_k(x)$ and a time dependent T-periodic function $h_k(t)$ [16], i.e:

$$\Sigma_k = \{x \in R^n / \sigma_k(t, x) := s_k(x) - h_k(t) = 0\} \tag{3-30}$$

The s_k functions can take any form because these are the product between feedback coefficients and the variable error signals. In this study, we have three control functions: s_1, s_2 and s_3 and three T-periodic functions h_1, h_2 and h_3. Every time s_i signal and h_i ramp cross with each other, a switching moment σ_k is registered. Each ramp h_i crosses the respective s_i control signal twice per period. This is the reason why the subindex i in the control signals s_i and the ramps h_i is changed by the subindex k in equation (3-30).

In the case of digital controller, the only value that cares is the first one each control signal take at the beginning of each period. This value is maintained until this actual period ends. Once the time moments in which these intersections take place are found, it is possible to get stationary average values and desired switching period T for the state variables.

$\sigma(X^*, \tau^*)$, which must be equal to zero, is defined as follows:

$$\sigma(\tau^*, X^*) = \begin{pmatrix} K_i(I_{ref} - i_L) - K_{v1}(\frac{1}{3}V_{IN} - V_{C1}) - h_1(t_{n(1)}) \\ K_i(I_{ref} - i_L) - h_2(t_{n(2)}) \\ K_i(I_{ref} - i_L) - K_{v3}(\frac{2}{3}V_{IN} - V_{C2}) - h_3(t_{n(3)}) \end{pmatrix} \tag{3-31}$$

where the t suffix **n** depends on the duty cycle in steady state: If it is between 0 % and 33 % $n = [1, 2, 3]$, if duty cycle between 33 % and 66 % $n = [3, 1, 2]$ and if duty cycle between 66 % and 100 % $n = [2, 3, 1]$.

X^* is given by equation (3-32) which is explained in the next subsection. A root finding algorithm should be applied to equation (3-31) to obtain $\tau^* = (t_1^*, t_2^*, t_3^*)$. For this study it was used the **fsolve** Matlab function.

3.3.4 Fixed points

A fixed point of P is a point X^* in the state space for which we have $X^* = P(X^*, \tau^*)$. Using the expression for P, X^* can be expressed in terms of the vector of steady state time durations τ^*, corresponding to the fixed points X^*, and matrices ϕ, ψ evaluated at τ^*. For *open-loop* systems, the time durations vector is already given so the next equation is used to obtain it [27] [16].

$$X^*(\tau^*) = (1 - \phi(\tau^*))^{-1}\psi(\tau^*) \tag{3-32}$$

It is important to notice that the fixed point and its associated M-modal periodic orbit exists and its unique whenever the inverse in equation (3-32) exist, i.e. if the matrix $(1 - \phi(\tau^*))$ is not singular, only one solution for the switching equations may exist and there will be just one fixed point, open-loop system would be linear.

For the *closed-loop* case, once the root finding algorithm is applied for equation (3-31) and the vector of intersections in time is obtained, the fixed points can be found with equation (3-32). The root finding algorithm will make sure the intersections between control signals and ramps are made, the duty cycles are obtained when forcing the system to have the same variable values for the $(n+1)T$ than for nT. Once this duty cycles are obtained, must be applied to equation (3-31) and the vector τ will be obtained.

3.3.5 Orbital stability analysis

The stability of periodic orbits x^* is the same as it is for fixed points X^* of the map P. This can be investigated with the Jacobian matrix DP of the map P. This matrix reveals the effect that very small perturbations near the fixed point X^* have at the end of the same cycle. The fixed point and the periodic solution will be stable if the eigenvalues of DP lie inside the unit circle.

As the system is piecewise affine time invariant, it is possible to obtain the DP in closed form in terms of t_k. In *open-loop*, as the time moments are previously given in a fixed pattern, DP can be expressed as the product of the Jacobian matrix of each local map. Differentiating equation (3-20) with respect to the discrete state variables x_n, the Jacobian matrix DP can be obtained as:

$$DP = \phi(\tau) = \prod_{k=M}^{1} \phi_k(t_k) \tag{3-33}$$

The asymptotic stability of the system will be assured if each affine configuration is asymptotically stable , which means that if all the matrices A_k have their eigenvalues in the left side of the complex plane, all the eigenvalues of $\phi(\tau)$ will be inside the unit circle [27] [16].

In order to perform the orbital stability analysis for the *closed-loop*, let us consider the values for the parameters given in section 3.2:

With this parameters a stable behavior is obtained and the switching sequence can be expressed as follows:

$$Co_1 \rightarrow Co_2 \rightarrow Co_3 \rightarrow Co_4 \rightarrow Co_5 \rightarrow Co_6 \tag{3-34}$$

corresponding to $(u_1, u_2, u_3) = (1,0,1), (1,0,0), (1,1,0), (0,1,0), (0,1,1), (0,0,1)$ and giving a rise to a 6-modal periodic orbit in the stationary state.

In order to analyze the stability of this orbit, the local behavior of the map **P** in its vicinity must be studied. The expression of the Jacobian matrix is modified by the presence of terms containing the derivative of the vector of switching instants τ with respect to the vector of the discrete state variables x_n. The expression for the Jacobian matrix in closed-loop systems is:

$$DP = \phi(t) + \frac{\delta P}{\delta d_i}\frac{\delta d_i}{\delta x_n} \tag{3-35}$$

If the open-loop system is stable, the second term in the new Jacobian matrix equation is the one that introduces instability in the system. By adjusting the parameters and making them as small as they can be, it is possible to solve this problem for the closed-loop system.

There is another method which consist on replacing all the duty cycles d_i equivalents, directly into the Poincaré map P expression in equation (3-20). As a result, the Poincaré map expression will depend now on the variables and the Jacobian matrix can be now obtained easier by using the next expression:

$$DP = \frac{\delta P}{\delta x} \tag{3-36}$$

From here, it is possible to work either with the normal model given by the matrices A and B (equation (2-8)) or the dimensionless model (equation (3-8)). In order to make the calculations a little bit simpler, an approximation is done. This approximation is explained next:

Poincaré map approximation

In this section, an approximation for the Poincaré map expression is taken in order to make it piece-wise linear [21] [28] [29]. This approximation is shown in the following equation :

$$e^{At} \approx I + At \tag{3-37}$$

which means the new Poincaré expression is given by:

$$x_{n+1} = (I + AT)x_n + BT \tag{3-38}$$

The main purpose of using this approximation is to simplify the discrete time model. By doing this, the period orbits stability analysis is also simplified because this way, it is much more simple to do the mathematical calculations related to stability.

When the new Poincaré expression in equation (3-38) is used, there are changes in the figures obtained. The approximation is good enough to be used in order to detect the first bifurcation.

In order to do the analysis that corresponds to the approximated model and to obtain the Jacobian matrix, the A and B matrices in equations (2-8) are taken. These matrices depend on the duty cycles d_1, d_2 and d_3.

As mentioned before, one of the methods to obtain the Jacobian matrix, consists on replacing the equivalent of the duty cycles equations (2-7), which depend on the variables in the vector x, into the A and B matrices. Then, replace these new matrices into the poincaré map approximation equation in (3-38).

To obtain the Jacobian matrix, it is necessary to define the new P expression. Using equation (3-26), the next affirmation can be done:

$$P = x_{n+1} = \begin{bmatrix} x_{1,n+1} \\ x_{2,n+1} \\ x_{3,n+1} \end{bmatrix} \tag{3-39}$$

This new expression will depend only on the variables, which in this case will be called x_1, x_2 and x_3, and are part of the variable vector x. As the whole new poincaré map expression depend

on x, the Jacobian matrix can be obtained applying equation (3-36).

$$DP = \frac{\delta P}{\delta x_n} = \begin{bmatrix} \frac{\delta x_{1,n+1}}{\delta x_{1,n}} & \frac{\delta x_{1,n+1}}{\delta x_{2,n}} & \frac{\delta x_{1,n+1}}{\delta x_{3,n}} \\ \frac{\delta x_{2,n+1}}{\delta x_{1,n}} & \frac{\delta x_{2,n+1}}{\delta x_{2,n}} & \frac{\delta x_{2,n+1}}{\delta x_{3,n}} \\ \frac{\delta x_{3,n+1}}{\delta x_{1,n}} & \frac{\delta x_{3,n+1}}{\delta x_{2,n}} & \frac{\delta x_{3,n+1}}{\delta x_{3,n}} \end{bmatrix} \tag{3-40}$$

The variables values are replaced by the fixed points X^*, which are obtained with equations (3-32). They vary depending on the parameters values, which in this case will be k_i.

$$DP = \begin{bmatrix} 1 - \frac{V_{in}Tk_i}{L} - \frac{RT}{L} & \frac{k_{v1}x_2T}{L} - \frac{Tk_{v1}(\frac{v_{in}}{3} - x_2)}{L} & \frac{k_{v3}x_3T}{L} - \frac{V_{in}k_{v3}T}{L} - \frac{Tk_{v3}(\frac{2v_{in}}{3} - x_3)}{L} \\ \frac{Tk_{v1}(\frac{V_{in}}{3} - x_2)}{C_1} & 1 - \frac{k_{v1}x_1T}{C_1} & 0 \\ \frac{Tk_{v3}(\frac{2v_{in}}{3} - x_3)}{C_2} & 0 & 1 - \frac{k_{v3}x_1T}{C_2} \end{bmatrix} \tag{3-41}$$

Then, the eigenvalues λ of the matrix obtained are obtained using the following expression:

$$\det(DP - \lambda \mathbf{1}) = 0 \tag{3-42}$$

A sufficient condition for stability is that all the eigenvalues λ lie inside the unitary circle [21].

4 State space analysis

In the electronic converters field, it is important to analyze the circuit variables behavior through time. It allows to understand how the parameters changes affect the circuit. They are the ones that define the dynamic system state.

There is always an initial state for the variables. The next variables values depend on the last values and so on. The most common thing to do, is to fix zero as the initial condition; even though, the system stabilization time depends on the initial conditions set: if the variables are close to the reference value, the system control will make the system stabilize sooner than if the initial conditions were far or zero.

In order to fulfill the requirements to obtain almost no ripple in the voltage of the capacitors and current in the inductor, the following values for the circuit elements were taken. Besides this, these parameter values make the system control response more efficient. The dimensionless parameters given in the expressions in eq. (3-6) , have elements which take the values specified as follows:

$$\begin{aligned} &R = 10\Omega \\ &L = 1mH \\ &C_1 = C_2 = 22\mu F \\ &V_{IN} = 1200V. \end{aligned} \tag{4-1}$$

The circuit with this parameter values will be called for now on **reference circuit** in order to make the analysis more organized.

There are other parameters that can modify the behavior on the circuit by changing their magnitude, these are the feedback coefficients k_{v1}, k_{v2} and k_i. The main reason to change them is to compare the system response, and also to see which are the best values for each one in order the system behavior is stable.

The feedback coefficient values taken for the reference circuit analysis were:

$$k_{v1} = k_{v2} = 0.01 \qquad k_i = 0.05 \tag{4-2}$$

Using the control signals (2-3) and the feedback coefficient adjusted to the values previously set, the control response shown in figure **4-1** is obtained with the algorithm made in MATLAB.

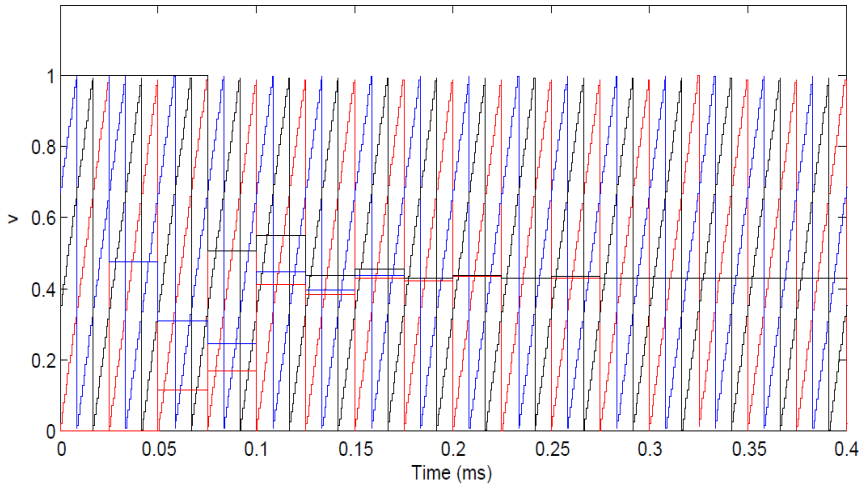

Figure 4-1: Control response - Algorithm

Figure **4-1** is compared to one obtained with PSIM simulator in figure **4-2**. Both graphics show the same control response, they are similar, take the same time to stabilize in the same value, which is 0,44 V. This value is also the switches duty cycle for the reference circuit after transient.

In both figures **4-1** and **4-2**, there is a saturation function and it is the one that makes the control signal to be 1 or 0 when they take values higher than 1 or lower than 0. The new signal take the upper or lower value depending on the case.

The variable values obtained with the Matlab algorithm for this same parameters are the ones in figure **4-3**. They can be compared to the ones in figure **4-4**, which are the ones obtained with the simulation software PSIM. Both graphics are similar, the transient takes the same time, the difference is that the MATLAB algorithm just plot the first value each variable takes per period and PSIM has registered all the values the variables take through time.

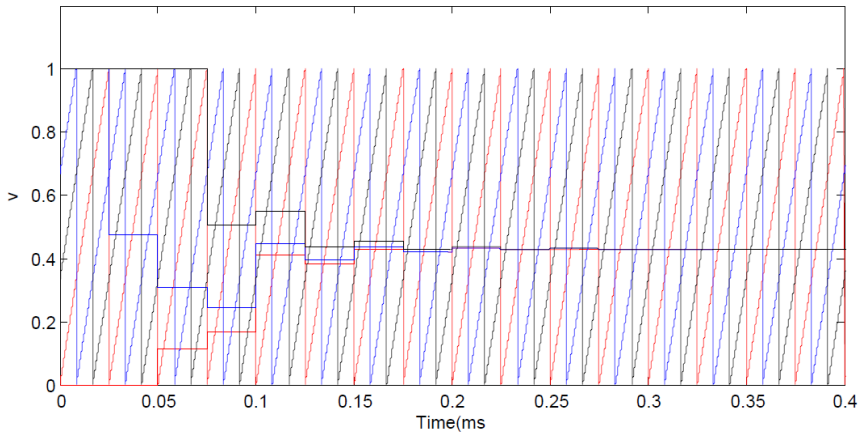

Figure 4-2: Control response - PSIM

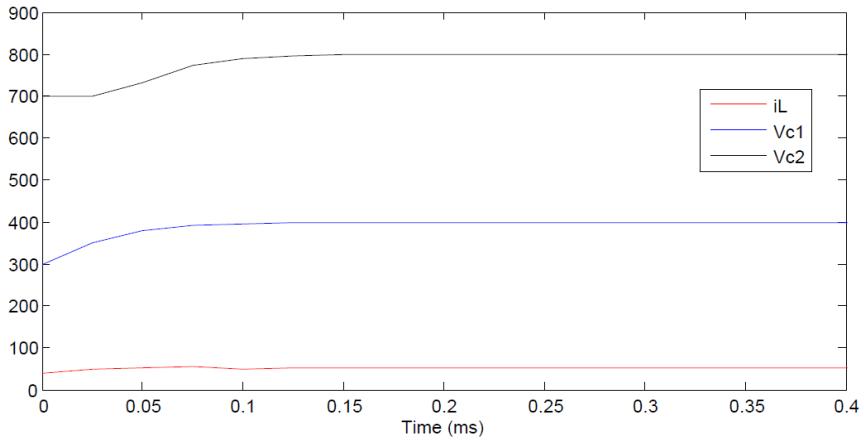

Figure 4-3: Variables behavior - Algorithm

In both figures **4-3** and **4-4**, it is possible to see how the control works. The capacitors voltage reference is achieved and even when the current reaches a value lower than the one expected which is 60 A, the circuit has a stable behavior.

In order to explain in a more complete way the circuit behavior, the system answer when the parameter values change are shown and analyzed in the following section.

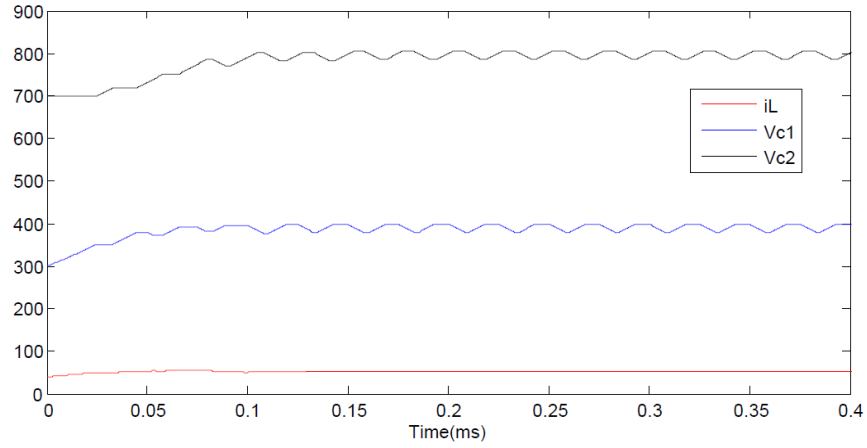

Figure 4-4: Variables behavior - PSIM

4.1 Change in resistor value

When there is a change in the resistor value, and this one is decreased, it can be observed that the lower the resistor value goes, the lower the value the control signals take when stabilizing. If the values taken by the control signals get lower, the duty cycles present the same reaction because this one is equal to the time the switch remains in **ON** state. This means that the control signal will be higher than the respective ramp for longer.

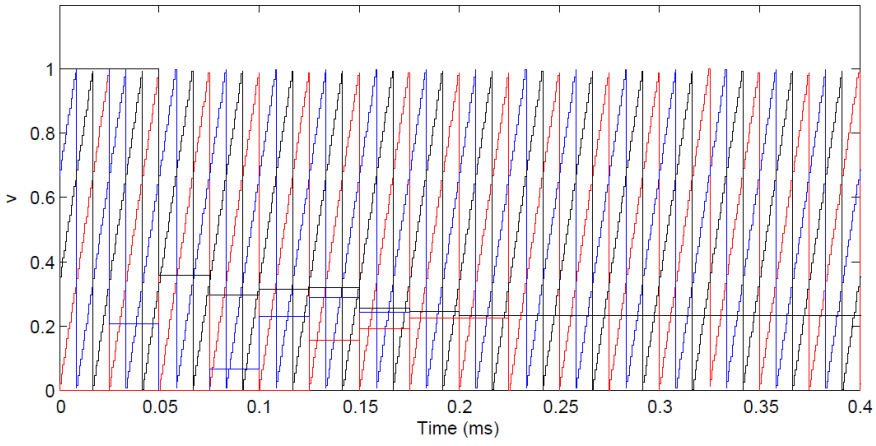

Figure 4-5: Change in control signals when R is decreased.

Changes in the control signals most of the times mean changes in the variable values. In this case, the variables are affected just a little, the values change but the voltages error signals do not. The current changes its behavior: when the resistor value is smaller, the transient is now bigger, the reference is not reached either. It still exist an error signal but this one is smaller.

In the figures **4-5** and **4-6** are the images that supports the information given above. Both figures obtained with the algorithm developed in MATLAB with a resistor value R=5Ω.

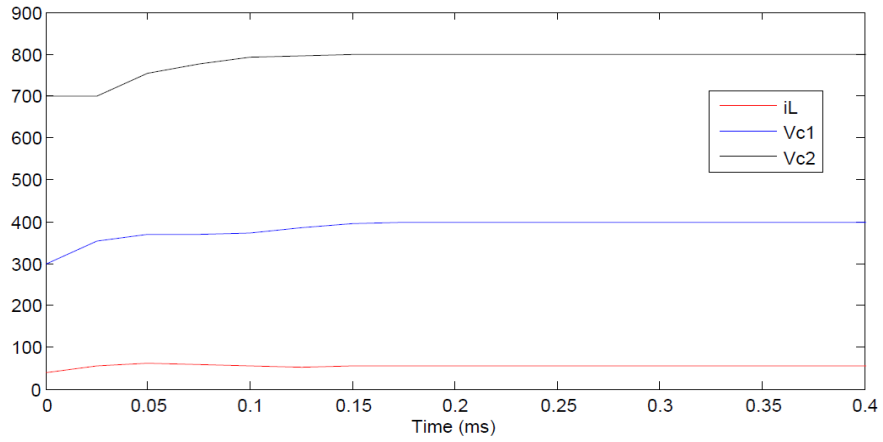

Figure 4-6: Change in variables when R is decreased.

If the resistor value is increased, the control signals stabilize in higher values. If the resistor takes a value that is greater, the circuit control may take too long to stabilize the system, the transient part will be too big, and if this value is very high, then it may never get stable. Some of the control signals will not be able to obtain a value between 0 and 1 and they will be continuously trying to get closer to 1 until eventually they do it. When some of the control signals s_k are higher than 1, their duty cycles are 1, which means that are all the time in **ON** state.

In the case of the capacitor voltages, it takes more time for them to achieve the reference value. The transient is then directly proportional to how high the resistor is. For the inductor current, there is an error signal but it can be easily seen that the variable answer is slower in comparison to when the resistor value was 10 Ω.

From the figures **4-7** and **4-8** the analysis above was taken with R=16Ω.

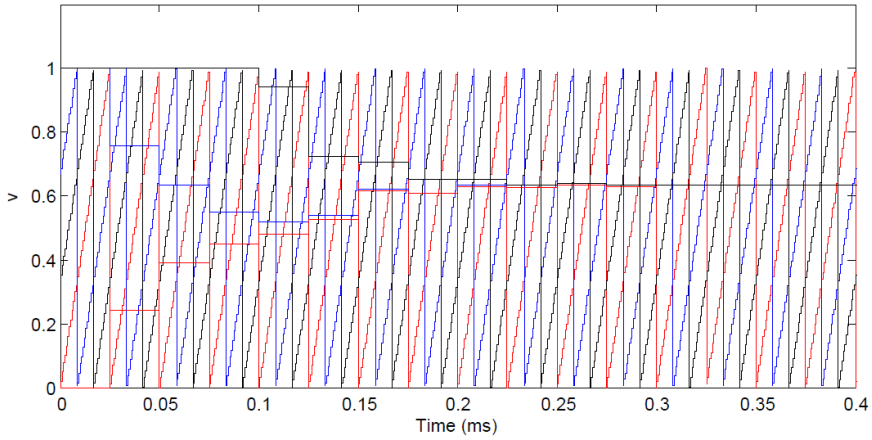

Figure 4-7: Change in control signals when R is increased.

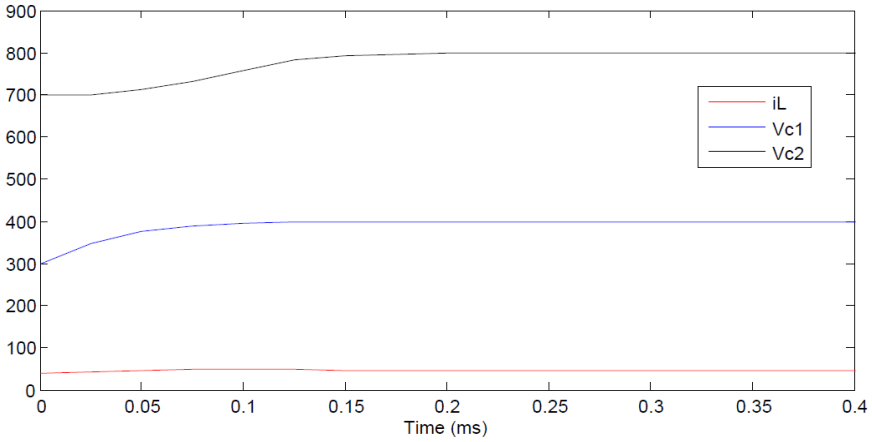

Figure 4-8: Change in variables when R is increased.

4.2 Change in the inductor value

If the idea is to modify the inductor value, it is important to pay attention because it may cause that the system change from continuous to discontinuous. If the inductor value is decreased, the system takes more time to stabilize and the variables take more time to achieve the reference value, in other words, the transient time is bigger.

The figures **4-9** and **4-10** show the behavior of the control signals and variables respectively. An inductor 0.8 mH was used.

As concluded, when the inductor value decreases, the transient time increases. Following this

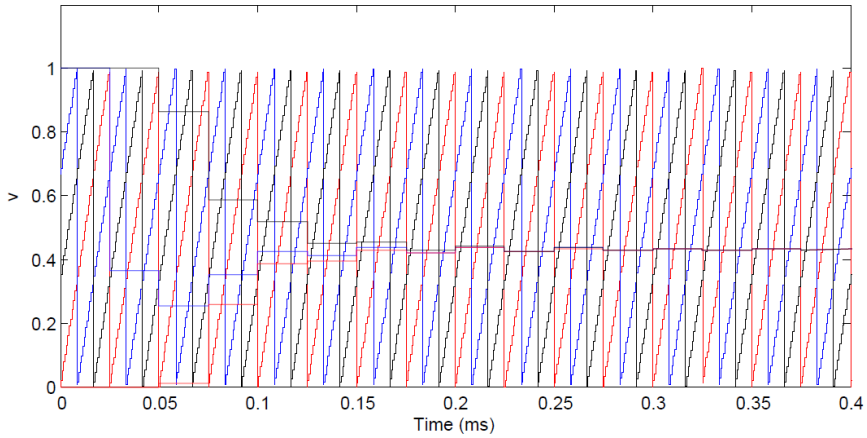

Figure 4-9: Change in control signals when L is decreased.

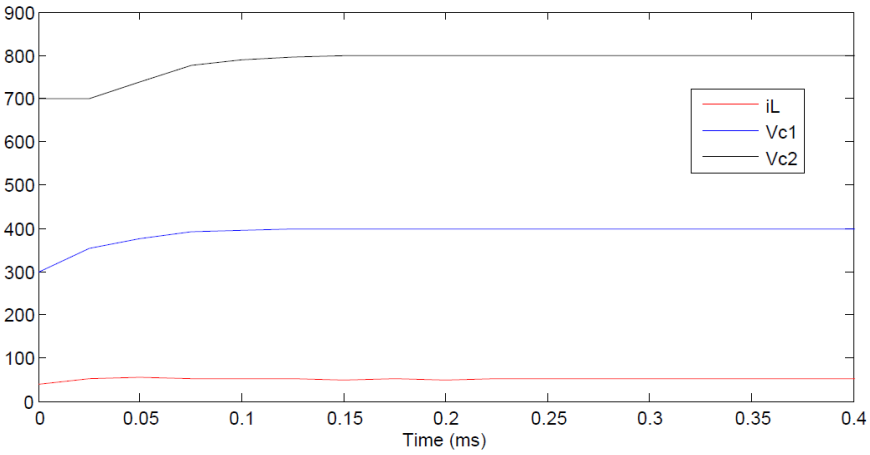

Figure 4-10: Change in variables when L is decreased.

logic, one should say that this time the transient will decrease, but what really happens is that the transient does not increase, but it does not decrease either. It is almost the same. This change affects the variables behavior, they take more time to achieve the value where they stabilize, this can be seen in figure **4-12**.

The duty cycles are not affected by the inductor value. The value where the control signals stabilize is equal for any inductor value tried in this study: 1 mH, 0.8 mH or 2 mH.

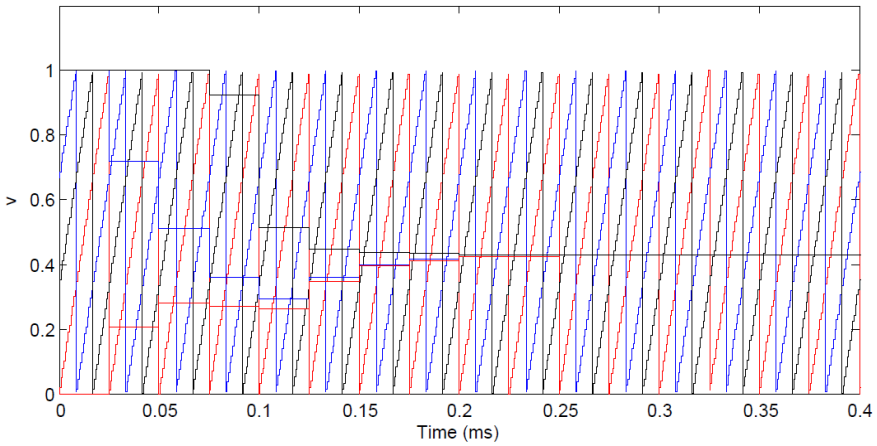

Figure 4-11: Change in control signals when L is increased.

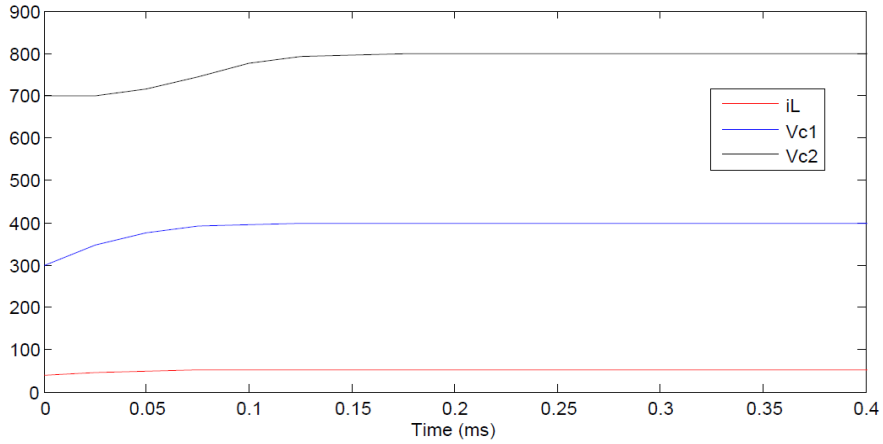

Figure 4-12: Change in variables when L is increased.

4.3 Change in the capacitors values

When the capacitors values are decreased, for example to 10 μF, the system response would be equal to the one obtained with the reference circuit. The duty cycles are not affected, the value in which the control signals stabilize would be approximately the same one in the basic configuration.

Even though, it might be a problem with a smaller capacitor, if it is really small the circuit becomes unstable.

The figures **4-13** and **4-14** show the circuit behavior: control signals and variables in time respectively.

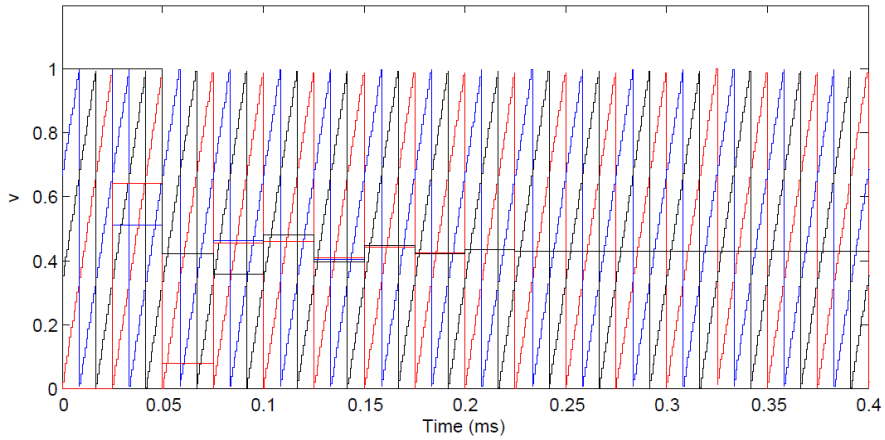

Figure 4-13: Change in control signals when C is decreased.

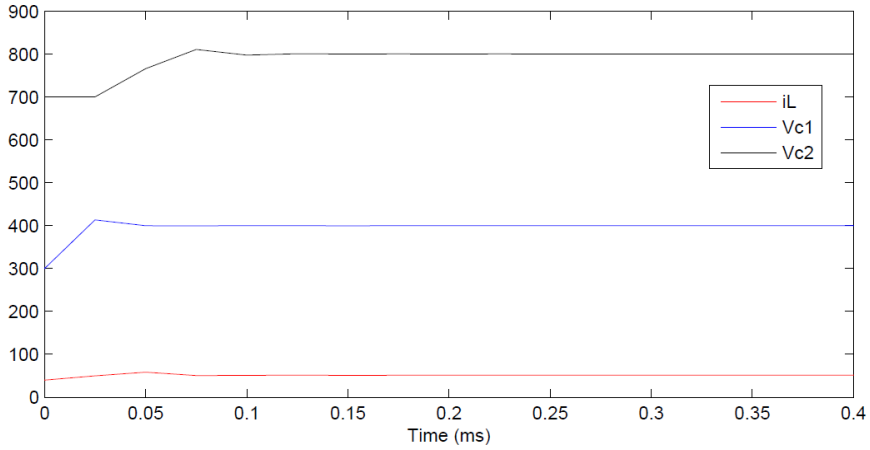

Figure 4-14: Change in variables when C is decreased.

When the capacitors take a greater value, for example 33 μF, the circuit transient increases as well. The variables do not achieve the reference value as soon as they do when using a 22 μ capacitors which is the one used in the reference circuit. The duty cycles are not affected either. The ripple in the capacitor voltages is smaller, which is good, but the transient increases.

The previously described behavior can be seen in figures **4-15** and **4-16**.

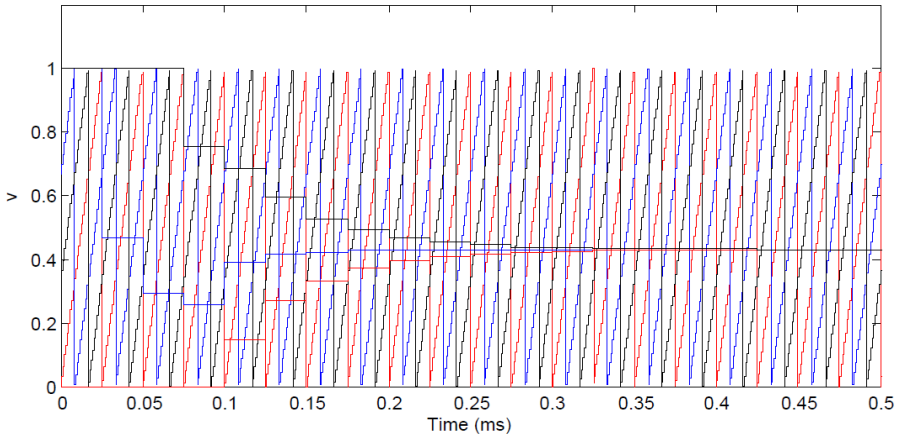

Figure 4-15: Change in control signals when C is increased.

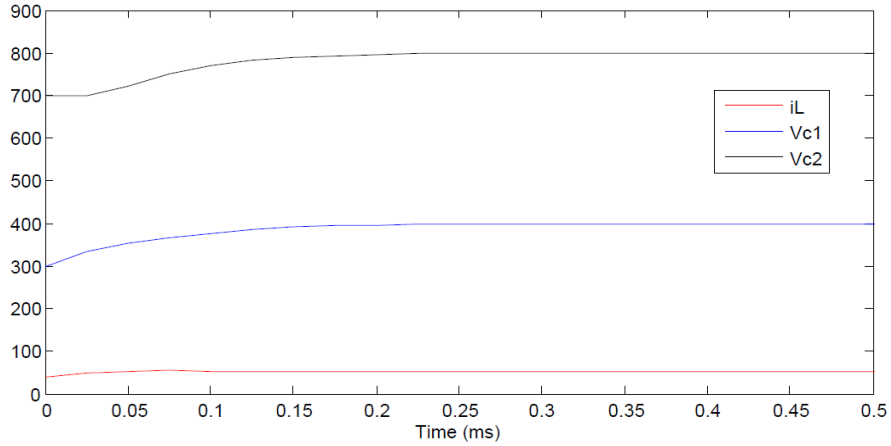

Figure 4-16: Change in variables when C is increased.

5 Nonlinear dynamics

In this section, the system bifurcation behavior is analyzed. As defined in [30], the qualitative changes in the dynamics of a system are called **bifurcations**, and the parameter values at which they occur are called **bifurcation points**. In this study, to get the bifurcation diagrams the parameter to vary will be k_i; also for each bifurcation diagram, three different k_i values will be taken and the variable. Duty cycles figures for each one of them will be obtained in order to support and make a deeper analysis of the system behavior.

As k_i is the main parameter and is the one that is varied in this study, the most interesting phenomenon will be appreciated in the current bifurcation diagram. The other diagrams will show how the other variables are affected by these changes, even though the dynamic is different because it depends on the tolerance taken for each variable.

For the diagrams in chapter 5 and also in chapter 6, the parameters were taken as is was stated in chapter 4, eq. (4-1) and the reference current was $I_{ref} = 50A$.

5.1 i_L Analysis

Figure **5-1** presents the bifurcation diagram for the current of the three-cell buck converter while the parameter k_i is varied from 0.04 to 0.15; the I_{ref} value taken is 50 A because it is possible to see the interesting behavior the current takes.

It can be easily seen how at the beginning, the current presents a stable behavior. There is a single value curve which represents a fixed point until $k_i \approx 0.68$, which is when there is period doubling. This period doubling continues until the k_i reach the approximate value 0.078, that is when the current signal i_L takes four different values for a short time and then chaotic behavior is registered. Later, this chaos stabilizes in four periods between $k_i \approx 0.103$ and $k_i = 0.107$. At this last point, the branches bifurcates again and an eight period domain starts; when $k_i \approx 0.12$ period becomes infinite because the current shows a continual variation in amplitude.

In this case, bifurcation occurs as the k_i parameter is increased.

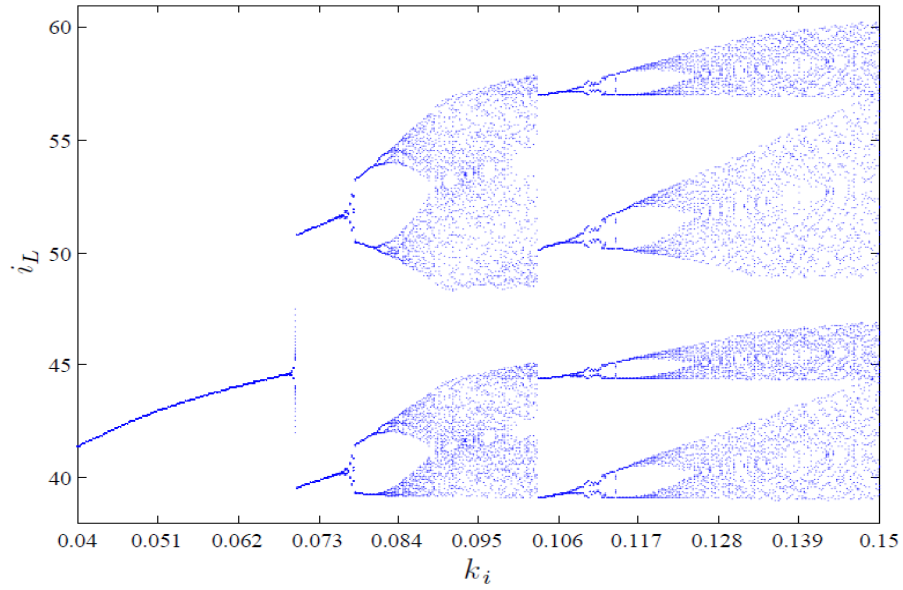

Figure 5-1: Bifurcation Behavior for i_L when k_i is varied.

There is an analysis for the current behavior when giving different values to k_i.

$k_i = 0.06$

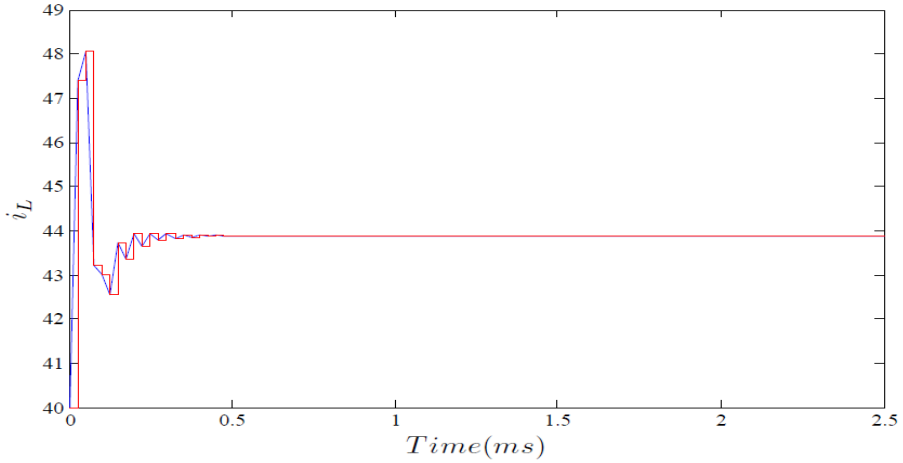

Figure 5-2: i_L behavior for $k_i = 0.06$

Figure **5-2** describes the current behavior for $k_i = 0.06$. In this sketch, it is possible to see that the transitory is short in time. The variable i_L stabilizes in a lower value than the one expected which is $I_{ref} = 50A$. The difference between the reference signal and the one obtained, is an error signal

that needs to be considered. The current can not reach the reference value for this given k_i.

Comparing this figure **5-2** with the bifurcation diagram in figure **5-1**, it is possible to predict that the value the current will take is approximately 44 A. This bifurcation diagram also allowed to predict the stability that is shown in figure **5-2**.

Figure **5-1** also predicts a stable fixed point when $k_i = 0.06$, which means the system is stable for this k_i value. This fixed point existence was proved with procedure explained in section 3.3.4. This way was demonstrated that both algorithms are accurate and the method used to get results works.

$k_i = 0.09$

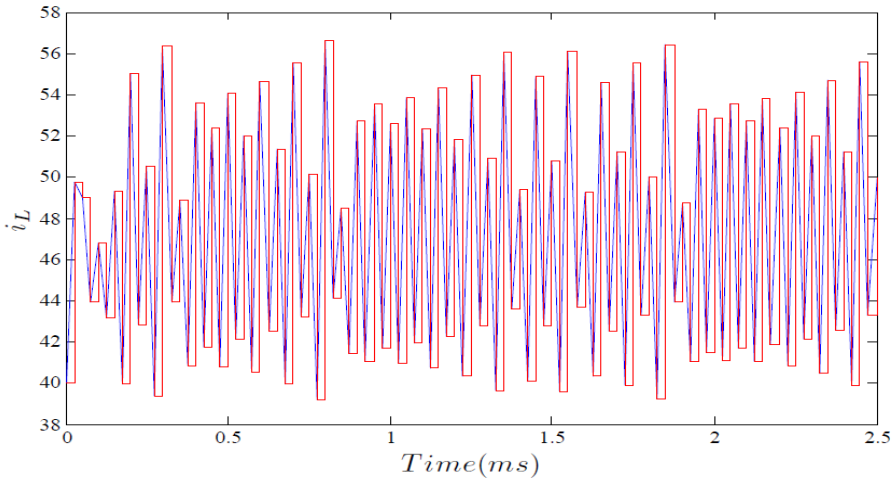

Figure 5-3: i_L behavior for $k_i = 0.09$

$k_i = 0.09$ is taken because of the dynamic behavior that can be seen in figure **6-1**. Both graphics **5-1** and **5-3** show that for this parameter value, it is supposed to be registered chaos.

At figure **5-1**, when $k_i = 0.09$, two chaotic important zones are described, this means that the current alternates the values it takes and never stabilizes.

Figure **5-3** describes the behavior for the current when $k_i = 0.09$, it is possible to see that there is no pattern or anything that indicates periodicity. The values vary in a wide range, so this figure indicates chaos, which confirms the conclusion made from figure **5-1** observation.

$k_i = 0.12$

The figure **5-4** describes the trajectory for the current i_L when $k_i = 0.12$. For this k_i value, in

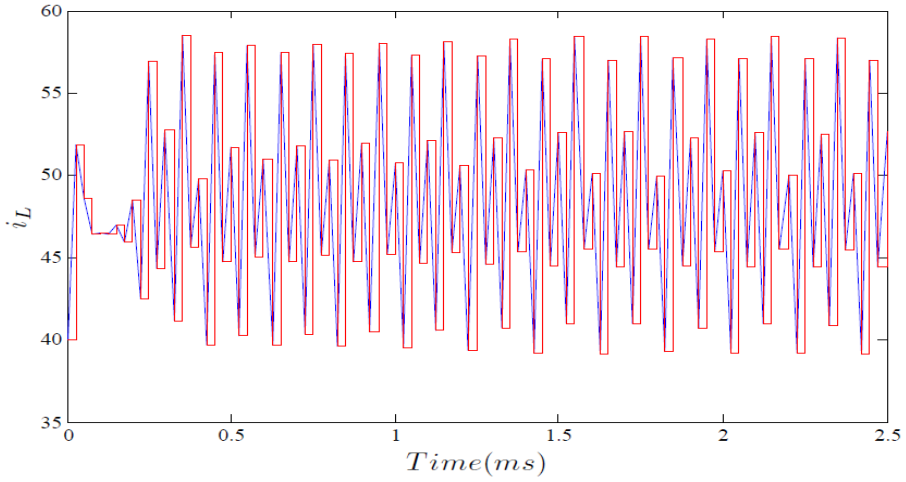

Figure 5-4: iL behavior for $k_i = 0.12$

figure **5-1**, there are registered eight subharmonics due to the existence of eight different branches, result of the bifurcation of four branches that appeared after a burst of chaos. Figure **5-4** is the proof of it, it can be easily seen that the red trajectory, which is the one that samples the first value per period, has different values after the transient, to be precise, eight different values.

The advantage of the current graphic registered as time increases, is that it is easy to recognize when the behavior is stable and when it is not. The magnitude is big but not as big as the voltages. For 3D bifurcation diagrams, one can think that the voltage does not vary as much as the current, but the truth is that it does vary. Those values have a bigger magnitudes, the difference looks like smaller but has to be considered.

5.2 V_{c1} Analysis

The control equations 2-3 given in section 2.2, show that for each capacitor voltage, there are corresponding feedback coefficients k_{v1} and k_{v2}. The parameter varied in the bifurcation diagram in figure **5-5** is k_i, which is the one that affects the current behavior. Even though, changes in the voltages are registered as well.

The bifurcation diagram for V_{c1} is shown in figure **5-5**. From this figure, it is possible to conclude that for k_i values between 0.01 and 0.062 approximately, there is a fixed point, there is a single value line and proves that it reaches the reference value. When $k_i = 0.068$, the output signal registers a continual variation in amplitude, so chaotic behavior is present for a very narrow range because this behavior changes for the next value k_i and suddenly becomes a period one cycle

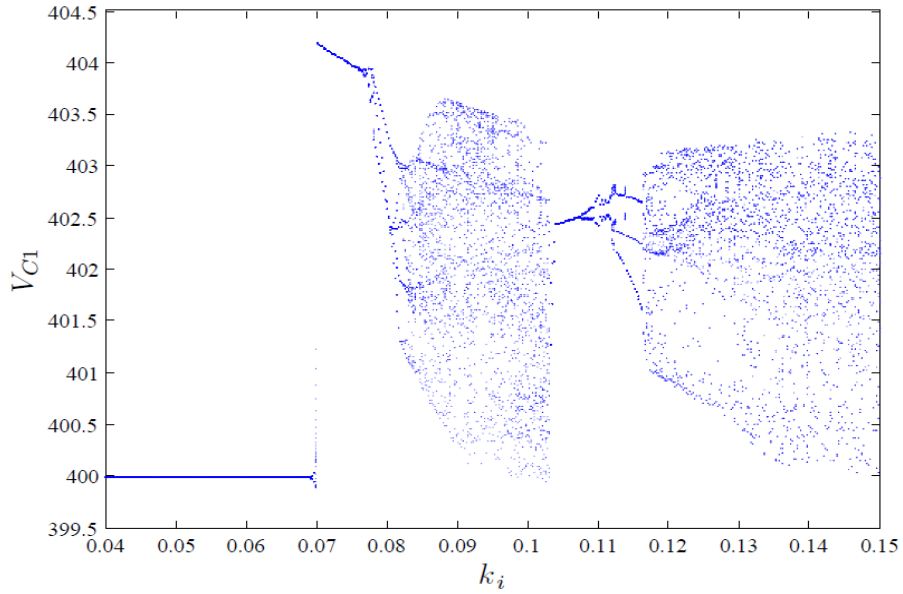

Figure 5-5: Bifurcation behavior for V_{c1}

which means that there is another fixed point but for this one, the value for this voltage is bigger than the reference. When k_i reaches 0.075, the variable starts to bifurcate until finally chaotic behavior appears. When $k_i \approx 0.1039$, the chaos stops and stable behavior starts again. As k_i gets bigger, bifurcation appears for V_{C1} values until another chaotic domain appears and this is the behavior that continues until the contemplated range of parameter k_i swept finishes.

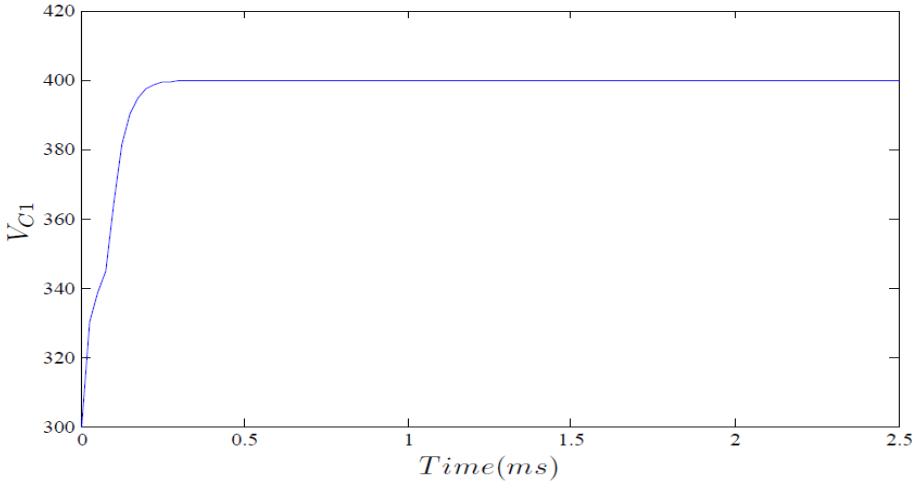

Figure 5-6: V_{c1} behavior for $k_i = 0.06$.

$k_i = 0.06$

The image **5-6** indicates that for $k_i = 0.06$, the reference voltage is reached once the transient ends. This signal is stabilized in 400 V, which is the voltage magnitude wanted. In the bifurcation diagram in figure **5-5**, it is shown that the voltage value will reach the reference once the transient ends. It is also possible to see that the voltage is stable and maintains its value, so it can be concluded that figure **5-6** supports the information plotted on the bifurcation diagram in figure **5-5**.

$k_i = 0.12$

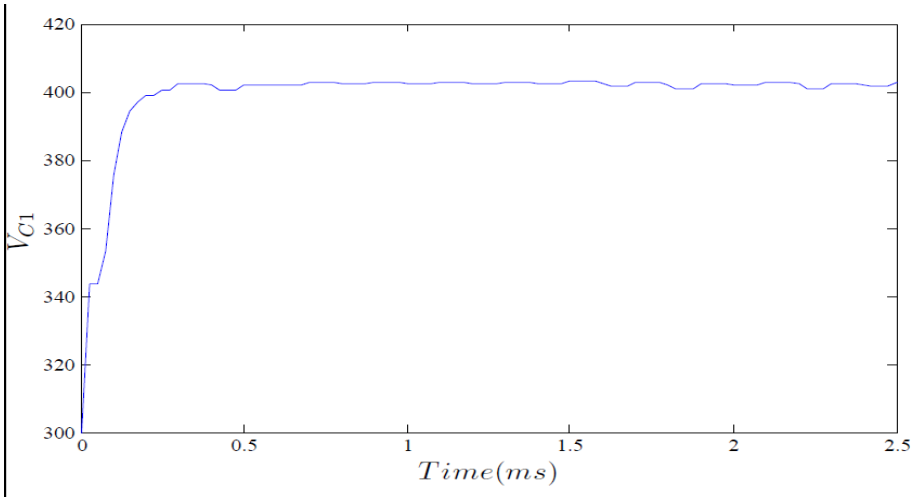

Figure 5-7: V_{c1} behavior for $k_i = 0.12$.

Figure **5-7** shows that for $k_i = 0.12$, the reference value for the voltage in capacitor 1 is near 400 V, even thought there is a ripple in the value obtained as a result, which can be seen easily. The behavior in this figure is the one that the bifurcation diagram showed for this k_i value. The ripple indicates that there is no stability, the word that better describes the behavior is chaos.

As mentioned before, this looks like a meaningless non linearity, but in fact it is an important one due to the magnitude of the variable values expected and registered.

$k_i = 0.15$

In figure **5-8**, it can be seen that the voltage does not take a stable value. It takes many values because of the presence of a ripple, and as this signal is sampled each period, each sample is different to the other. At least it is different enough to consider that there is an infinite period domain.

Even when in figure **5-8** it looks like the voltage value does not vary that much, it is important to notice that tolerance is different for voltages and this is the reason that the difference between values is apparently smaller in figure, but in magnitude is big enough to consider not stable behavior.

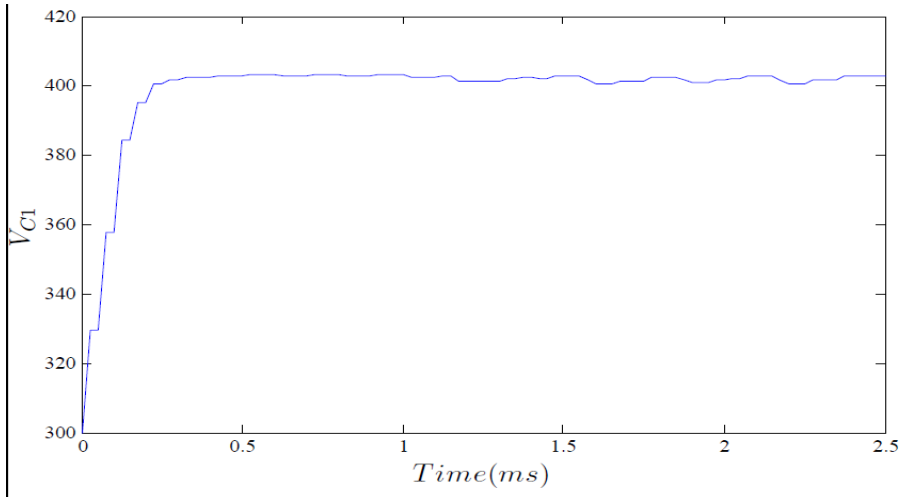

Figure 5-8: V_{c1} behavior for $k_i = 0.15$

The bifurcation diagram in figure **5-5** shows a wide range of values for V_{C1} when $k_i = 0.15$ and the infinite period domain can be confirmed.

5.3 V_{c2} analysis

Now, capacitor 2 voltage behavior will be analyzed. In figure **5-9** the bifurcation diagram for this variable is displayed. It can be seen that V_{c2} takes a value a little bit bigger than the reference value. When $k_i \approx 0.07$, the stable behavior stops, there is no longer a fixed point and the voltage magnitude is less than 798 V. As k_i gets bigger, the voltage magnitude increases, and also does the amount of subharmonics until infinite period domain can be easily seen.

When $k_i \approx 0.11$, chaos stops and one single branch is formed. This branch starts bifurcating and periodicity increases as well. A big chaos domain describes the values this variable takes for the last k_i parameter part of the swept.

$k_i = 0.06$
As shown in figure **5-9**, for a value of 0.06 in the feedback coefficient k_i, the voltage in capacitor 2 is the same of the reference value, which is approximately 800 V, and this can be proved with the figure **5-10**. This figure shows that after the transient, this variable takes this same value. The signal is stable, there are no ripples.

Both figures **5-9** and **5-10** indicate that there is a fixed point for this parameter values.

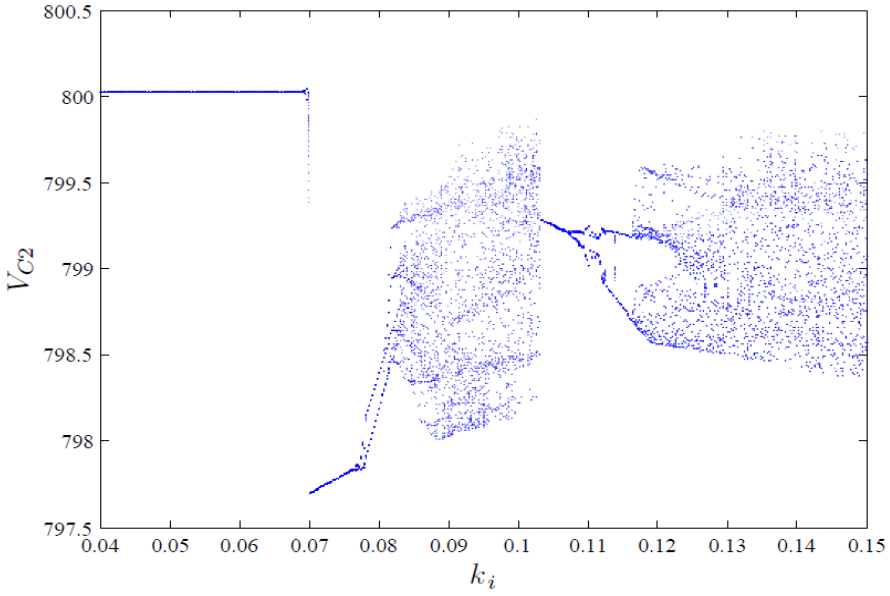

Figure 5-9: Bifurcation behavior for V_{c2}

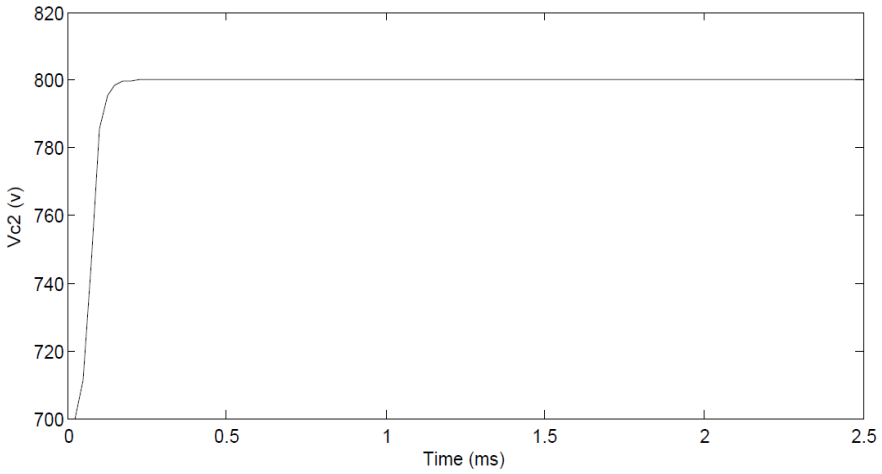

Figure 5-10: Voltage in capacitor 2 for $k_i = 0.06$

$k_i = 0.08$

In figure **5-11**, it can be seen that the voltage in capacitor 2 is approximate to 800 V, which is the reference value. Once the time is bigger, ripples appear destabilizing the voltage signal. There is an error signal generated by this ripple and in order to validate this behavior, in figure **5-9** there are registered different values for V_{c2} when $k_i = 0.08$ which means there is chaos.

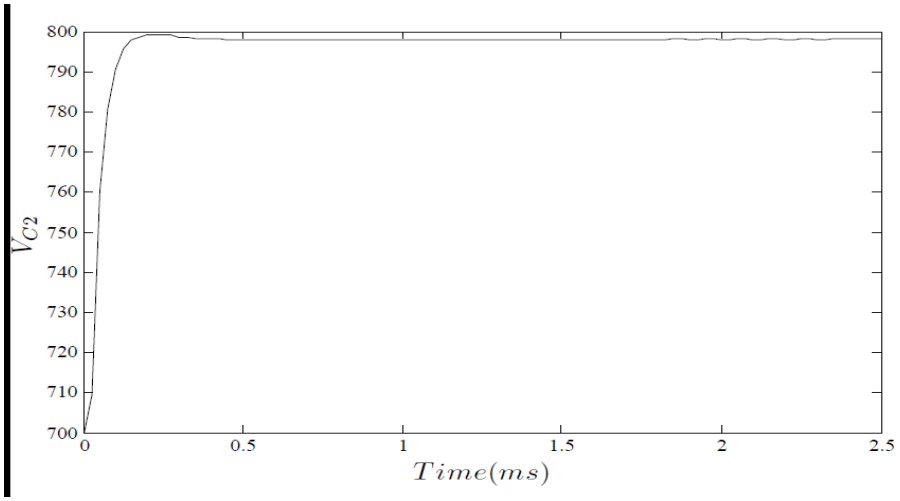

Figure 5-11: Voltage in capacitor 2 for $k_i = 0.08$

$k_i = 0.12$

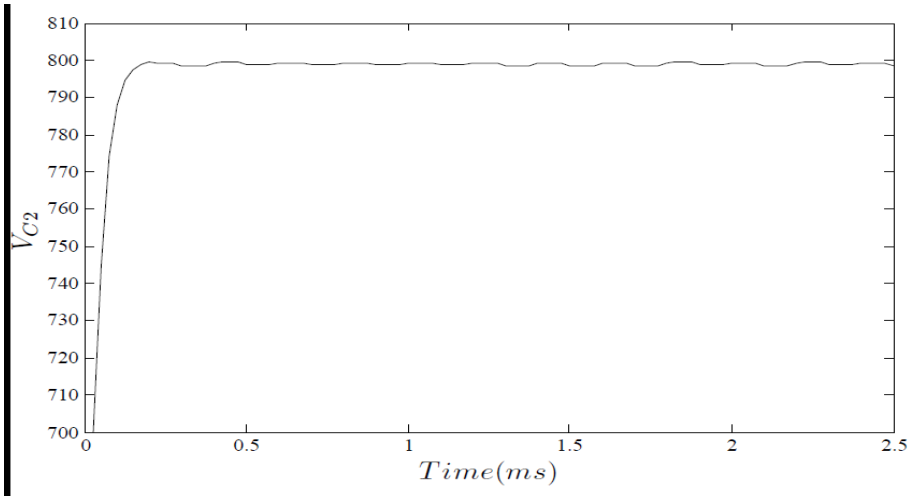

Figure 5-12: Voltage in capacitor 2 for $k_i = 0.12$

The figure **5-12** shows that for $k_i = 0.012$, the variable V_{c2} has a chaotic behavior due to the many values that the variable V_{c2} takes, as the time varies. It is possible to see that there is a small ripple and this ripple generates an error signal. For the voltages V_{c1} and V_{c2}, the bifurcation diagrams are different because they depend on the configuration that is running the buck converter and these voltages are increased, decreased or maintained. When the circuit changes configuration, the behavior in the variables may change as well, at least one of the behaviors change for sure (see chapter 2). In conclusion, it is not possible that the three bifurcation diagrams match, they present a different behavior in comparison to the bifurcation diagram for the current in the inductor i_L and

compared to each other as well.

As mentioned before, in the figures **5-11** and **5-12**, there is a ripple that proves the unstable behavior for the voltage in capacitor 2 when some k_i values are taken.
Figure **5-10** shows stability which proves this variable can be also stable when lower values for k_i are taken.

5.4 Duty cycles

The switches duty cycles are the time that each switch spends in an active (ON) state. The duty cycles are the pulse duration divided by the pulse period. In this section, the duty cycles are analyzed and compared for $I_{ref} = 70A$, their role in the three-cell buck converter is important because they are the ones that specify for how long the active configuration will be **ON**.

In the next subsections, the duty cycle behavior will be explained for three different k_i values. It will be possible to see how the duty cycles reflex the system behavior, just like it happens with the variables. In other words, it will be evidenced that if the variables are unstable, the duty cycles are not stable either.

$k_i = 0.06$
Through the duty cycles for the system when $k_i = 0.06$ (fig **5-13**), it can be observed that a stable value is taken after 0.6 mS. In this point, the system start switching from one configuration to another in a determined and fixed sequence:

$$C_8 \rightarrow C_3 \rightarrow C_2 \rightarrow C_7 \rightarrow C_5 \rightarrow C_6$$

This sequence happens once the requested state variables or time conditions are fulfilled. For a stable behavior, it is always expected that a sequence of configurations appear, even though this sequence depends on the switches duty cycles. As the sequence is the same and also are the duty cycles for the three switches, in the variables it is possible to see that there is a period one behavior.

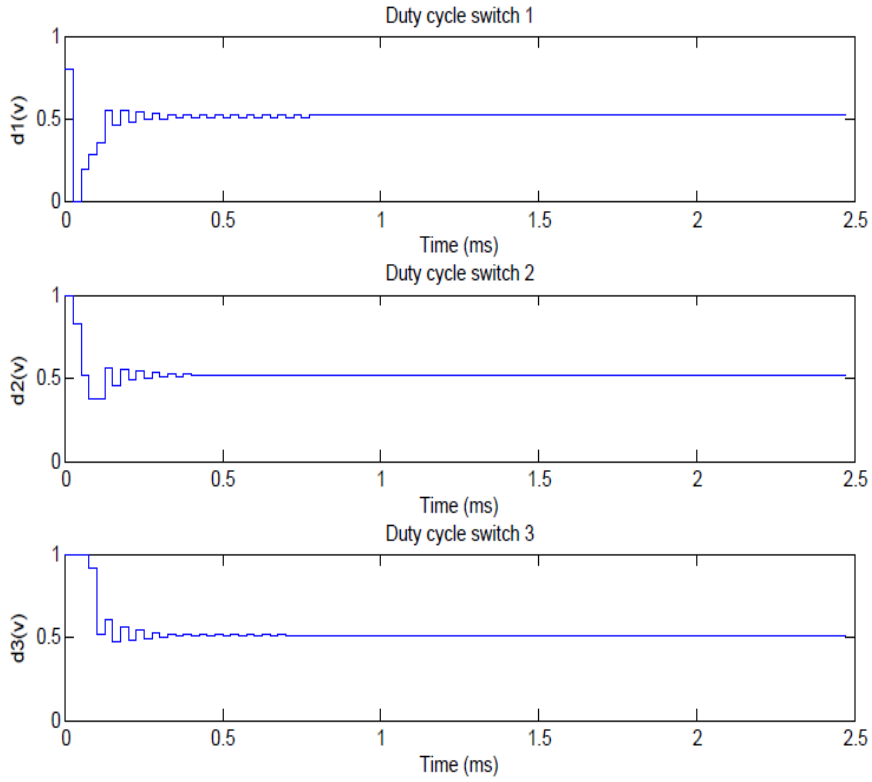

Figure 5-13: Duty cycles for $k_i = 0.06$

Figures **5-2**, **5-6** and **5-10** show that the control works because when the transitory for the state variables start in t $\approx$ 0.55 ms, the duty cycles have not been stabilized yet. The control changes in a way that the variables try to stabilize very fast and once this is accomplished, the duty cycles tent to stabilize as well.

$k_i = 0.12$
When $k_i = 0.12$, the system does not behave as stable. The variables do not take a particular value, they just take values that look like random but they are obtained through the control action. The variables have infinite period.

The three duty cycle signals in figure **5-14** for the first 0.1 ms behave in a different way. After this moment in time, they attempt to synchronize, these signals start to look alike because they take the same values. Despite the control efforts, they never stabilize and as a result the state variables do not stabilize either.

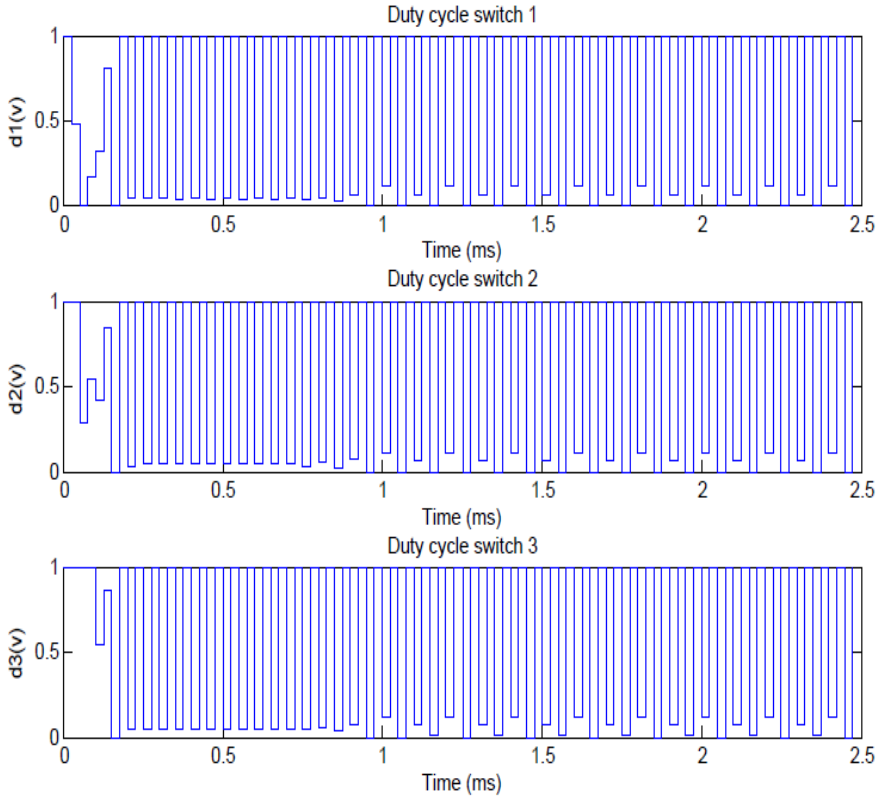

Figure 5-14: Duty cycles for $k_i = 0.12$

$k_i = 0.16$

For this value of k_i, and as reference current $I_{ref} = 70A$, the duty cycles do not stabilize. The state variables do not do it either and chaotic behavior is registered everywhere because the period becomes infinite due to the tolerance that was set. It is possible to see how the duty cycles sometimes take values 1 and 0. This means that the saturation control functions work perfectly when the control signals s_i take values that are too high or too low.

Just like it happens for $k_i = 0.12$, the duty cycles in figure **5-15** look alike, they start taking the same values approximately after 0.1 ms, even though the duty cycles vary so much per period that is not possible to recognize how many periods they have, this can be interpreted as if the period becomes infinite which is also considered as chaos.

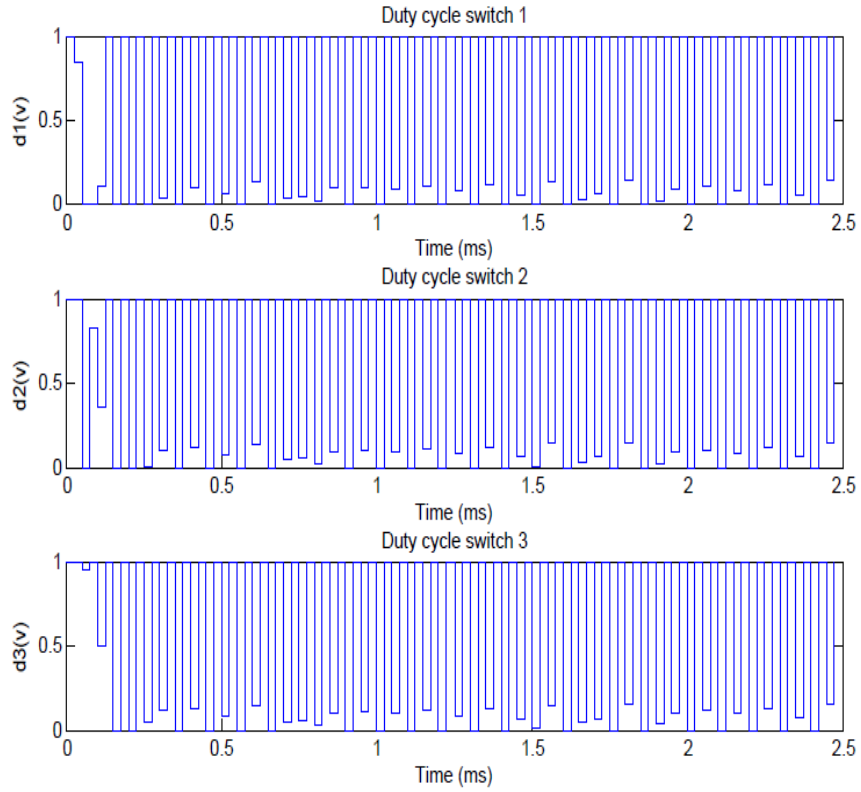

Figure 5-15: Duty cycles for $k_i = 0.16$

Diagram approximations

- i_L **bifurcation diagram**

When fig. **5-16** is compared to fig. **5-1**, it is possible to see that both figures describe a similar current behavior as k_i increases. Both have a stable first zone, which differs in the bifurcation point moment. For fig. **5-1**, the current i_L shows a stable behavior until $k_i \approx 0.068$, where period doubling is registered. For the diagram that was obtained using the approximation fig. **5-16**, the period doubling is registered for $k_i \approx 0.058$.

Such a difference is expected due to the effect of neglecting the non linear terms in the approximated form. Even though, as mentioned before, it is an acceptable approximation and allows to do the stability analysis. The main reason to work with the approximated one is to gain computational time. This technique has been used for other circuits analysis and has shown results that are in favor of its use [28] [18].

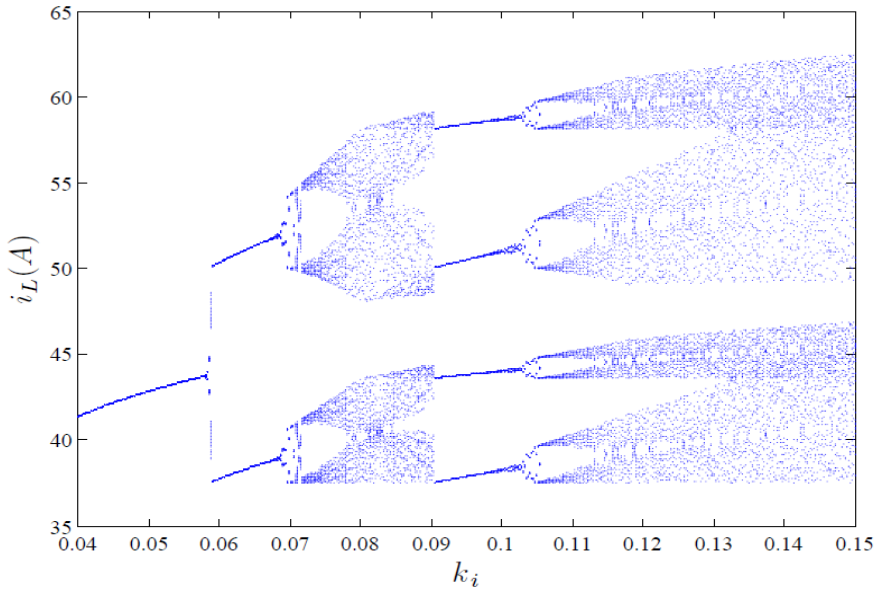

Figure 5-16: Bifurcation Behavior for i_L when k_i is varied with PWL Poincaré approximation.

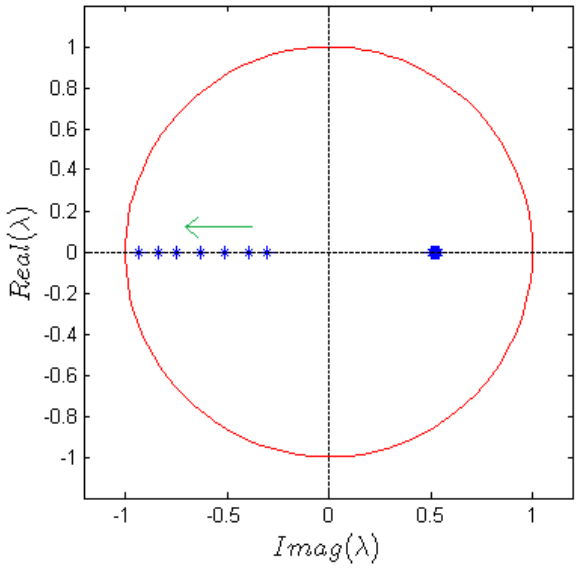

Figure 5-17: Stability analysis. Eigenvalues

For this case, where $I_{ref} = 50A$, the fig. **5-17** describes the trajectory the eigenvalues of the Jacobian matrix have as the k_i parameter is increased, to say it on a different way, when the stability stops. As mentioned before, a necessary condition for stability is that these eigenvalues lay inside the unit circle. The idea then is to obtain some eigenvalues

for $0.04 \leq k_i \leq 0.055$, which will prove the behavior is stable. Also, the eigenvalues for $k_i > 0.6$ will be obtained in order to prove that after this point, there is no stability, concluding that way that the bifurcation can be detected.

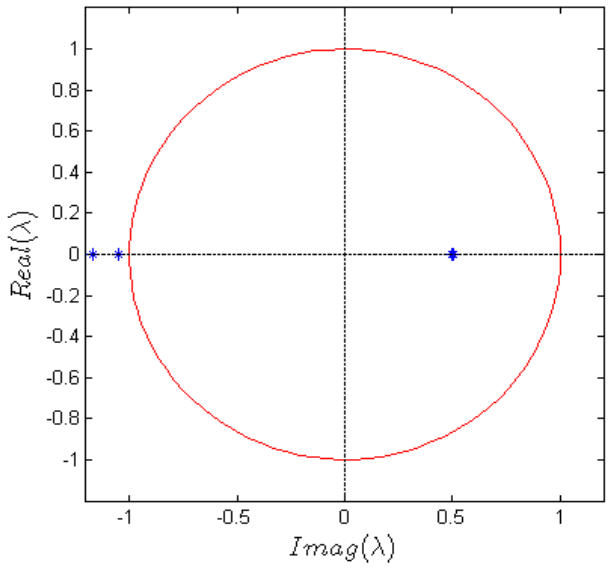

Figure 5-18: Stability analysis. Eigenvalues

In the fig. **5-17**, it can be confirmed the stability of the periodic orbits. All the eigenvalues plotted, are the ones for $0.04 \leq k_i \leq 0.055$. The green arrow indicates that as k_i is increased, the eigenvalues (represented by an asterisk "*") increase as well. As the range taken is still in the stable part, this is the reason why all the eigenvalues plotted lie inside the unit circle.

The fig. **5-18** shows the eigenvalues obtained for $k_i = 0.06$ and $k_i = 0.064$. Once again, as k_i increases, the eigenvalues approximate more to the left side of the real axis and of course, do not lie inside the unit circle.

- V_{c1} **bifurcation diagram**

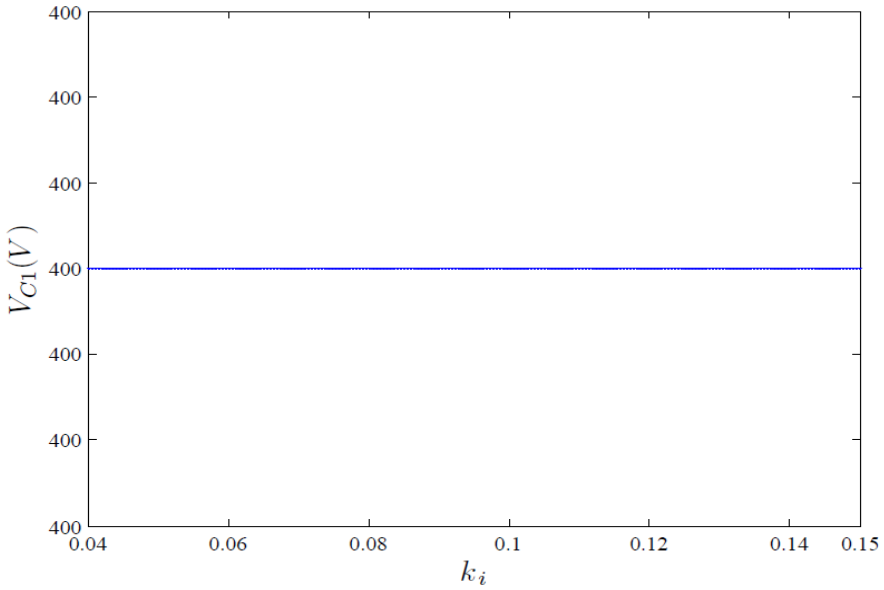

Figure 5-19: Bifurcation Behavior for V_{c1} when k_i is varied with PWL Poincaré approximation.

In the bifurcation diagram for V_{C1}, it is possible to see that the registered behavior is stable for all the values of k_i.

As mentioned before in this document, and of course, referring to some cited studies, it is possible to obtain this kind of differences between the approximated Poincaré map and the one that takes into account every single element.

In this case, the second and higher order terms in the P expression modify the behavior of the variables. When they are neglected, the bifurcation diagram show that at least the voltage in the capacitor take the value of the expected fixed points, which is $1/3$ and $2/3$ of V_{in}.

Most of the articles that work with the Poincaré map method, state that the non stability is a product of the second and higher order terms, which appear in the duty cycles expressions [21] [28] [29].

- V_c2 **bifurcation diagram**

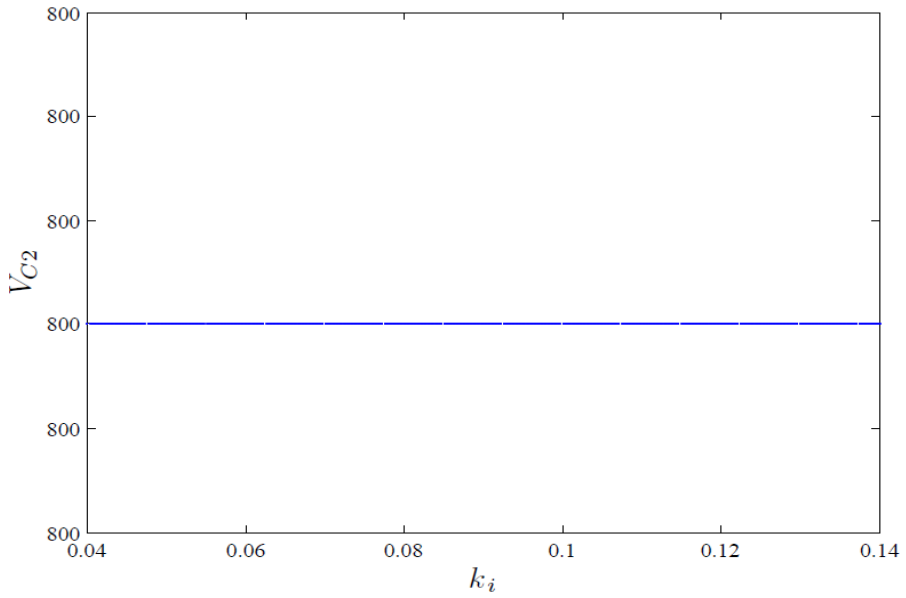

Figure 5-20: Bifurcation Behavior for V_{c2} when k_i is varied with PWL Poincaré approximation.

The bifurcation diagram for V_{C2} using the poincaré map approximation also presents the same behavior observed in the bifurcation diagram for V_{C1}. The variable take the reference value and maintains it as k_i increases.

As mentioned for the V_{C1} bifurcation diagram, this is due to the approximation, which neglects the second and higher order terms.

It can be concluded that an acceptable approximation of the bifurcation diagrams obtained with the Poincaré map expression in equation (3-20), are the diagrams obtained with equation (3-38). These last diagrams neglect second and higher order terms that appear in the duty cycle expressions. The behavior observed in the bifurcation diagrams can be proved with the periodic orbit stability analysis explained in section 3.3.5.

The Jacobian matrix and the corresponding eigenvalues were obtained, these could prove the veracity of the results and conclusions obtained with the bifurcation diagrams. The first bifurcation was successfully detected by using the approximated method.

6 Two and three dimensional bifurcations

In this section, there is a deeper variables behavior analysis using two dimensional bifurcations and 3D mesh graphs. Using these figures, it is possible to analyze the periodicity of the values taken by each one of the variables when parameters vary.

The images used in this chapter are obtained in two different ways, both related, but they represent the data differently: the first one is by plotting a matrix that contains the amount of different values per period that each one of the variables take once the transient has ended, of course, with a tolerance considered, not an absolute zero. This tolerance depends on the variable. The second procedure is to plot all the bifurcation diagrams together in order to see the values that each variable takes when the parameters are varied. As a result, a three dimensional graphic will be obtained and all the values each variable take per parameter combination will be shown. The procedure used to obtain the diagrams was poincaré map. Eventhough, the two-dimension diagrams are obtained using the poincaré approximation mentioned before.

As the current feedback coefficient is the one varied in the bifurcation diagrams, it is easy to deduce that directly affects the current signals. In order to get a behavior in two dimensions, first, as a second parameter must be varies as well. This can be the reference value for the inductor current I_{ref}. Next, there are obtained bifurcation diagrams where parameters I_{ref} and k_i are varied. The period behavior will be analyzed for each one of the variables and duty cycles.

The method used to obtain the periods per combination between k_i and I_{ref} is similar to the one used to obtain the regular bifurcation diagrams but has to be done may times for the different values of I_{ref}. The algorithm that allows me to obtain the bifurcation diagrams is modified so it does not plot a figure, it has to save the variables data in a matrix, the same data that would be plotted in a regular bifurcation diagram. These data are compared to each other and if they differ more than expected (varies more than the settled tolerance), a period is counted. This period increases when there is a considerable change in the analyzed variable behavior. e.g. If in the bifurcation diagram there is a stable part, this will be reflected in the two-dimensional diagram by plotting a blue region. If in the bifurcation diagram it is possible to see four branches for a given k_i, then in the two-dimensional diagram, in the same moment, a lighter blue region will be plotted. And, if in the bifurcation diagram, the values taken by the variable for a given k_i value are all very different,

and when counting the difference between them we obtain a periodicity of 15 or more, this will be represented with a red region, which means chaos.

6.1 Current in the inductor i_L

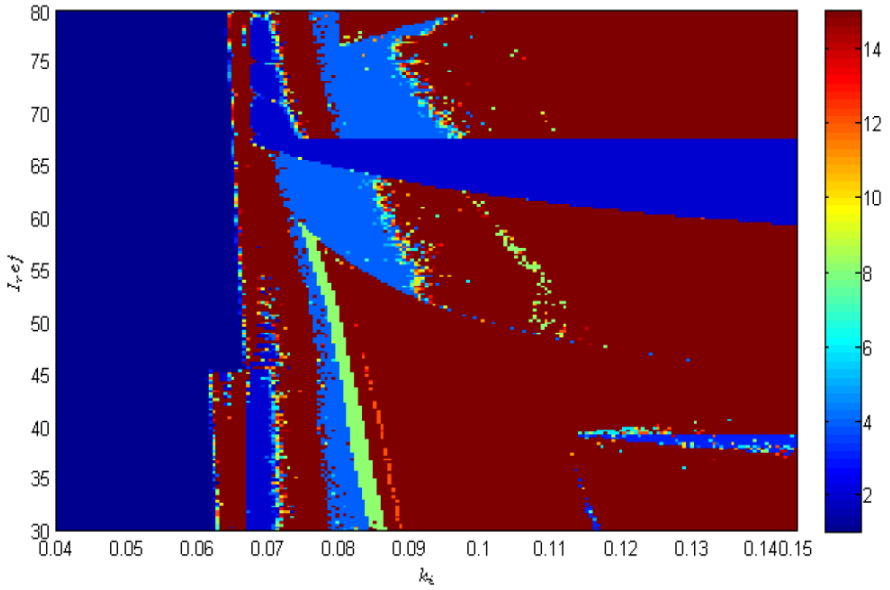

Figure 6-1: k_i Vs. I_{ref} periodicity for i_L

From figure **6-1**, it can be concluded that for values between 30 and 31.0101 A for the parameter I_{ref}, when k_i is varying, at the beginning there is a little area where non stable behavior is registered. Once the feedback coefficient k_i increases a little bit, the current behavior is stable for all I_{ref} take. After $k_i = 0.061$, non stable behavior is registered. There is no longer stability, and the two parameter map shows that there is a narrow range where the current values are represented with a short burst of chaos.

For the highest values of I_{ref}, there is intermittence in the behavior. There are parts where the current has a periodic behavior and then goes to chaos again. For lower values of I_{ref}, there are even more changes in the variable behavior. There are many chaotic domains that suddenly change to be $n-$periodic, where **n** is any number of periods that can be easily seen in the graphics. This happens for a very narrow range and then it goes back to chaos.

Figure **6-2** evidences the analysis made for the image **6-1**. It is possible to easily see that there is a big region where the current is stable. When $k_i \approx 0.065$, the one period zone becomes, for all the values that I_{ref} takes, chaos which is alternated with $n-$periodic behavior. For I_{ref} values

near 68 A, the current is stable for the first values of k_i. When this parameter is approximately 0.068, there is a chaotic domain which last for a very narrow range, up to $k_i \approx 0.073$ the variable remains stable.

For the other I_{ref} values, after the stable domain for the first values of k_i, there is a small chaos domain and after that the current is $n-$periodic, where **n** depends on the reference current I_{ref} value. After this, $n-$periodic domain chaos appears again. For some values of I_{ref}, the intermittence continues. For other values of I_{ref}, the chaos remains until k_i takes its last value which is 0.18.

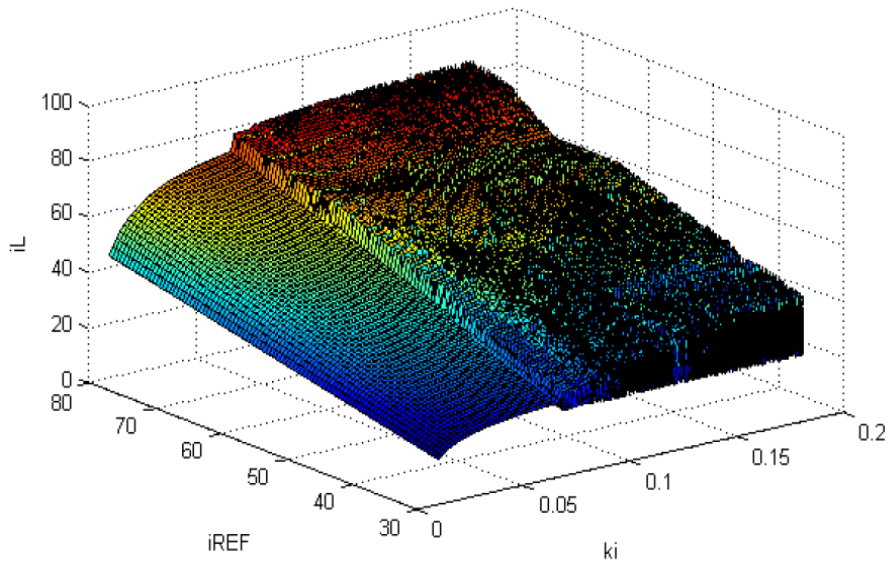

Figure 6-2: 2 parameter bifurcation diagram for i_L

Figure **6-2** only shows the values this variable takes, it is just like many bifurcation diagrams all together. It is possible to see how the value of the current increases as the reference current does. Also, for the stable first part, as k_i increases, the value the current gets bigger compared to the value that it takes for smaller k_i values.

Poincaré map approximation

The fig.**6-3** is the one that describes the 2 parameter bifurcation diagram obtained when using the approximation mentioned in section 3.3.5, equation (3-37).

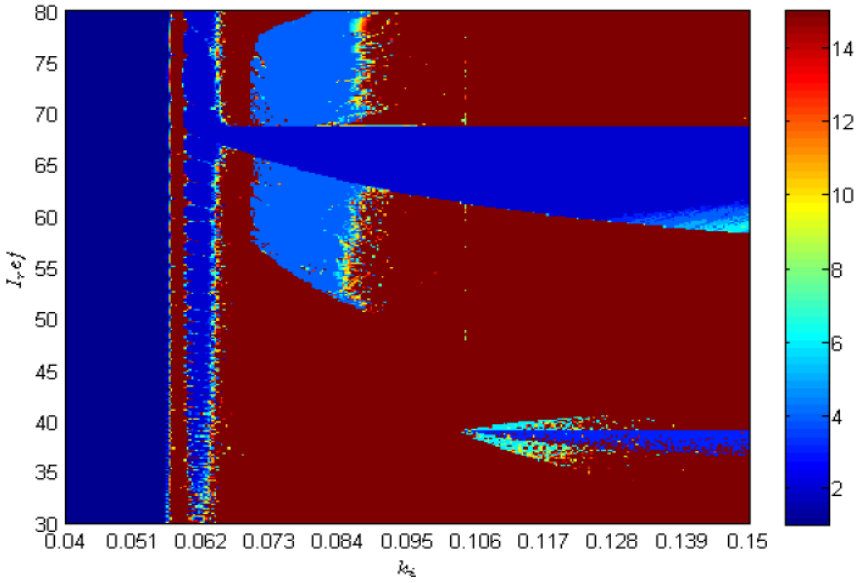

Figure 6-3: 2 parameter bifurcation diagram for current in the inductor

As it can be seen, there is a difference between the figure that uses the approximation and the one that does not. An interesting change is that in both of them, there is a period two zone. In the one that uses the approximation fig. **6-3**, it is possible to see that it presents phenomena that is similar to the one obtained in fig.**6-1**. The difference is because of the terms that are neglected, this diagram looks more stable or shows a more stable behavior when compared to the one with the complete Poincaré map. These two-dimensional bifurcation diagrams have the same important behaviors: For high values of I_{ref} and k_i between 0.8 and 0.9, there are two regions where it is reflected a period five for the i_L. There is another region, which is very small in diagram fig. **6-3** when compared to the one in diagram fig.**6-1** but is present in both figures: As k_i increases and $I_{ref} \approx 38A$, the number of periods decreases and there is an small but notable region with period two. After chaos, the periodicity and Fig.**6-3** is obtained in less time than it takes to obtain fig.**6-1**, which means that for more complex analysis where computational time is important, it is better to use the approximation method. Even when the bifurcation diagrams with and with no approximation are not exactly the same, the result is good enough to work with it.

It is possible to see that the limit between the stable behavior (1 period) and more periods zones, appears before. This means that the stable behavior changes before when using the Poincaré maps

approximation. This is also registered in the bifurcation diagrams for the current in the inductor.

6.2 Voltage in capacitor 1 V_{c1}

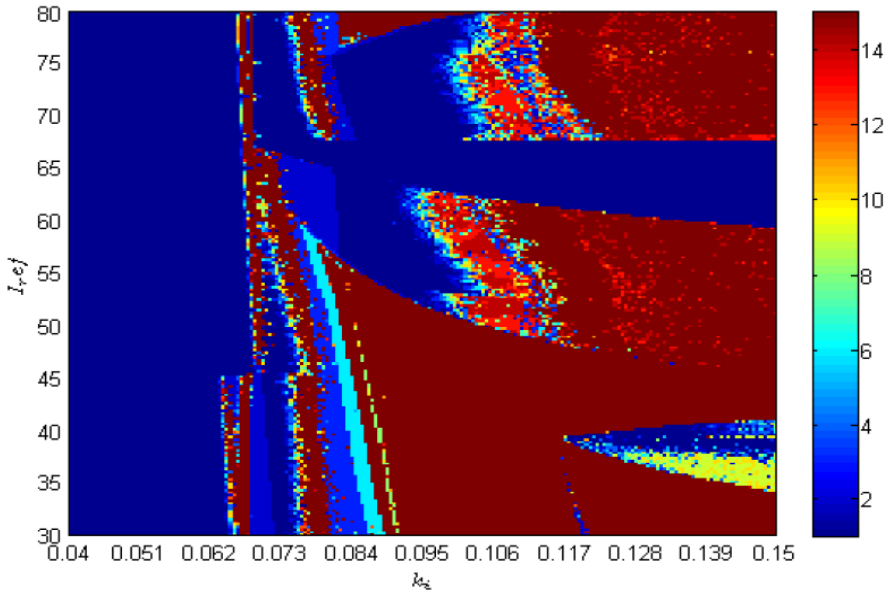

Figure 6-4: Periodicity diagram for V_{C1}

When parameters k_i and i_L are varied, V_{c1} is stable for a wide plotted area; this means that there are a lot of parameter combinations where there are fixed points. Most of it occurs for values lower than 0.062 for the current feedback coefficient k_i and for any value the reference current takes, making the exception of the lowest ones of $k_i \approx 0.017$, where there is n-periodic behavior for a very small region.

This two parameter map in figure **6-4**, is more dynamic than the one for the current in figure **6-1**; there are zones that are n-periodic instead of chaotic and just like in two parameter map for the current, for I_{ref} values near to 65 A, the variable behavior is stable but for narrow range near $k_i \approx 0.07$ where chaos is registered.

For I_{ref} values between 50 A and 80 A, and k_i values between 0.017 and 0.096, there is a domain where the stability is intermittent: for the lower values of k_i the voltage is stable, but after $k_i = 0.068$ periodic behavior or chaos domains are registered for a narrow range, then stable behavior appears again and later chaos or periodic domain appears. For k_i values between 0.096 and 0.123, and for I_{ref} higher values, there are two very dynamic domains and a stable one in the

middle: the dynamic domain presents a lot of different n-periodic behavior that can be obtained depending on the parameter combination.

An interesting behavior can be seen when I_{ref} is varied and $k_i \approx 0.18$: the current takes values that are intermittent between chaos, stability and period ten behavior.

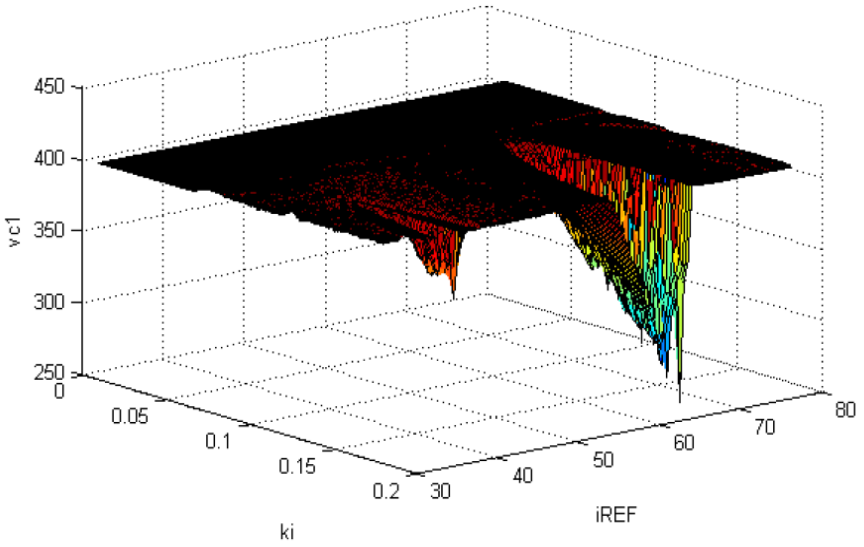

Figure 6-5: 2 parameter bifurcation diagram for V_{C1}

Some observations that can be made from the capacitor 1 voltage behavior are shown in figure **6-5**: there is an important non stable region where I_{ref} takes high values and k_i low values; it is clear that for I_{ref} values between 62A and 80A and for k_i between 0.116 and 0.138, V_{C1} takes lower values as the reference current signal increases being the lowest one 251,2V which is registered when $k_i = 0.1336$ and $I_{ref} = 80A$. The value this capacitor voltage takes depends on the reference current previously set; the control signals do not control this variable as they should in this non stable region, a difference bigger than the 10% of the reference value is not accepted for practical purposes.

Poincaré map approximation

Using the poincaré map approximation in equation (3-37), the fig. **6-6** is obtained. Comparing this figure to the one obtained with the regular poincaré map expression, fig. **6-4**, it is possible to observe that the phenomenon is not longer so similar and it does not behavior like the inductor current 2-parameter diagram. There is a big stable zones that covers almost all of the region except

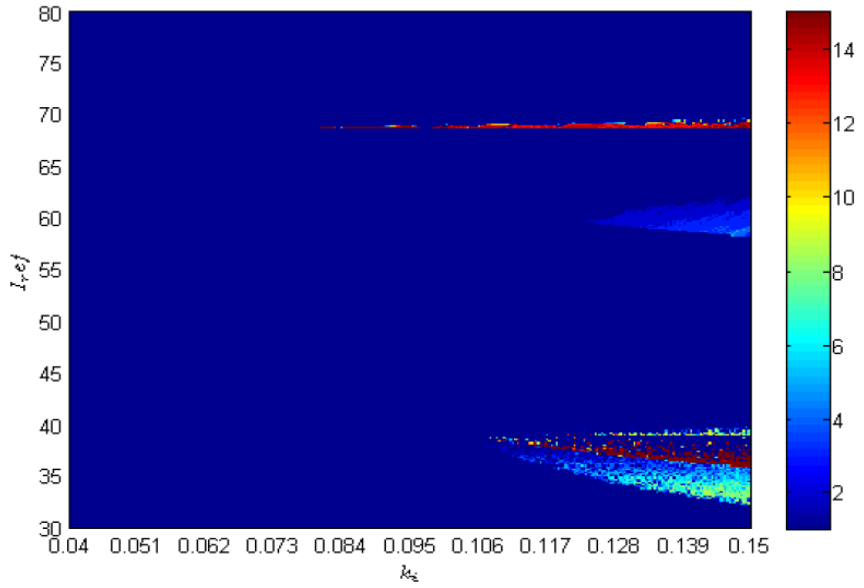

Figure 6-6: 2 parameter bifurcation diagram for Voltage in capacitor 1

for the higher k_i values and the lower I_{ref}.

6.3 Voltage in capacitor 2 V_{c2}

The voltage in capacitor 2 shows a behavior that is as dynamic as the one for capacitor 1; for the highest values of I_{ref} and for the first half of k_i values there is an intermittent behavior between stability and chaos. For some parameter combinations, the change between stability and chaos is slow, it means that the periodicity increases until chaos appears. This periodicity changes appear because of the continual variation in amplitude of the variable V_{C2}.

Just like it happens in the other variable two parameters map: for lower values of k_i, there is more intermittence than for higher values. In this case, the intermittence is between stability, six periodic behavior and chaos.

Also, there is a parameter combination for which the control does not work very well, it can be seen in figure **6-8** from $k_i = 0.101$ to $k_i = 0.138$ this variable takes values lower than the reference. This condition starts from $I_{ref} \approx 48A$ and for higher reference current values, the voltage in capacitor 2 gets lower and lower being the lowest value registered approximately 777 V.

In figure **6-8**, it is also possible to see the wide stable area for the first values of k_i, and through

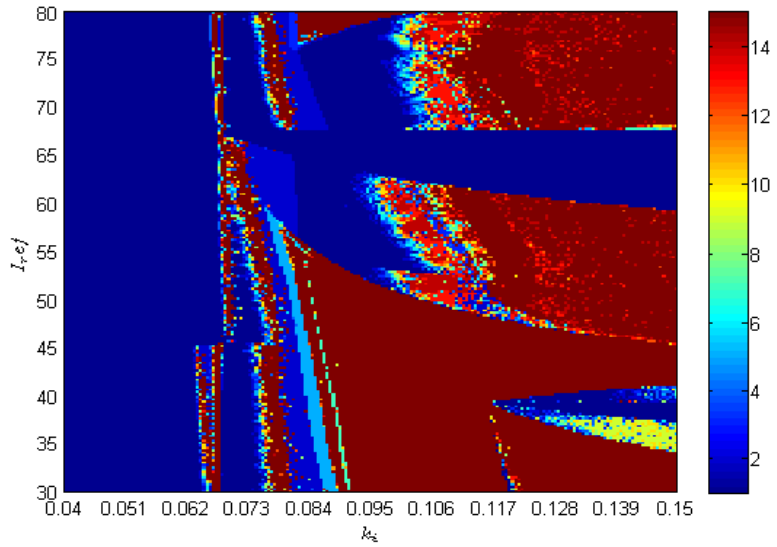

Figure 6-7: Periodicity diagram for V_{C2}

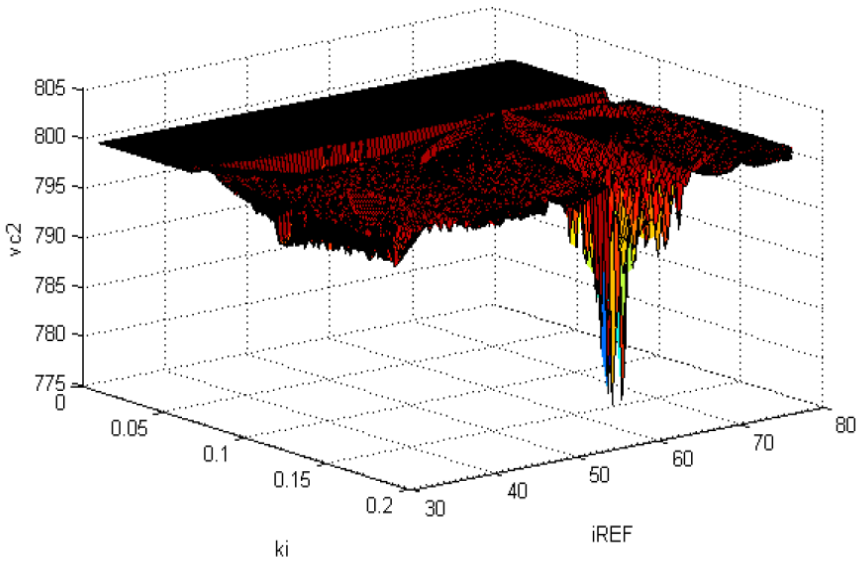

Figure 6-8: 2 parameter bifurcation diagram for V_{C2}

the Z axis it can be seen the different values the variable takes. The more values the variable take per parameters combination, the more periods it has and this can be easily proved with figure **6-7**, where periodicity for V_{C2} is shown.

Poincaré map approximation

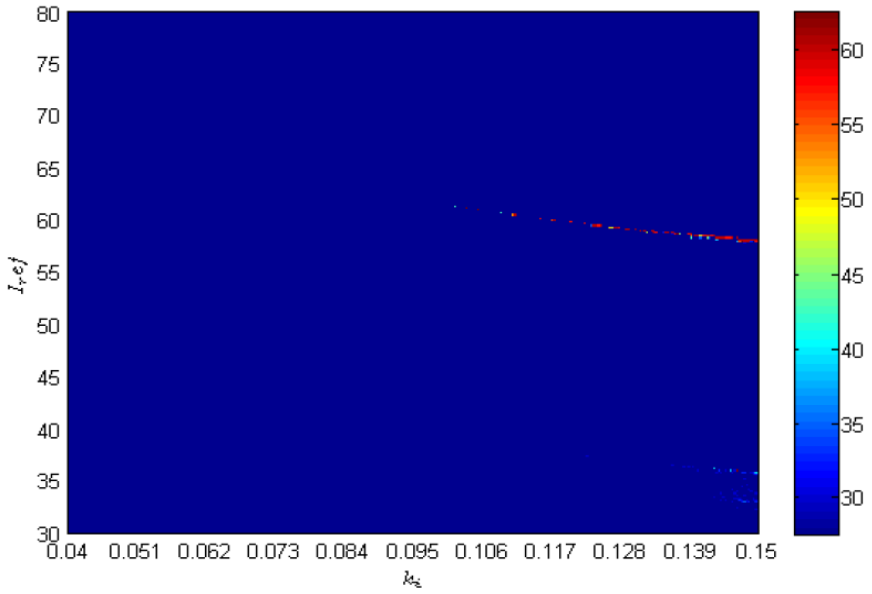

Figure 6-9: 2 parameter bifurcation diagram for voltage in capacitor 2

Figure **6-9** describes the two parameter bifurcation diagram with the approximated Poincaré method. For the voltage in capacitor 2, the graphic does change more. This graphic shows almost a complete stable behavior. It can be concluded that for the voltage in capacitor 2, the elements that add the chaotic or unstable behavior have two or more orders.

For both one and two dimensional bifurcation diagrams for voltage in capacitor 2, it has been possible to see that when the approximation is used, a more stable behavior is obtained. The instabilities that are registered in fig. **6-7** do not appear in fig. **6-9**.

6.4 Duty cycle for switch 1

For the switches duty cycles, a tolerance of $1x10^{-}6$ is considered to obtain the two parameter map.

If all the variables have a common stable domain, the most logic thing is that the duty cycles also have it. As it can be seen in figure **6-10**, a blue stable zone can be recognized in the left half. For k_i approximately between 60 A and 67 A, there is a domain of intermittent behavior: one periodic behavior appears, when I_{ref} is approximately 0.68 there is a narrow range of chaos, for some parameter combination in this range there is also n-periodic behavior where $n > 6$.

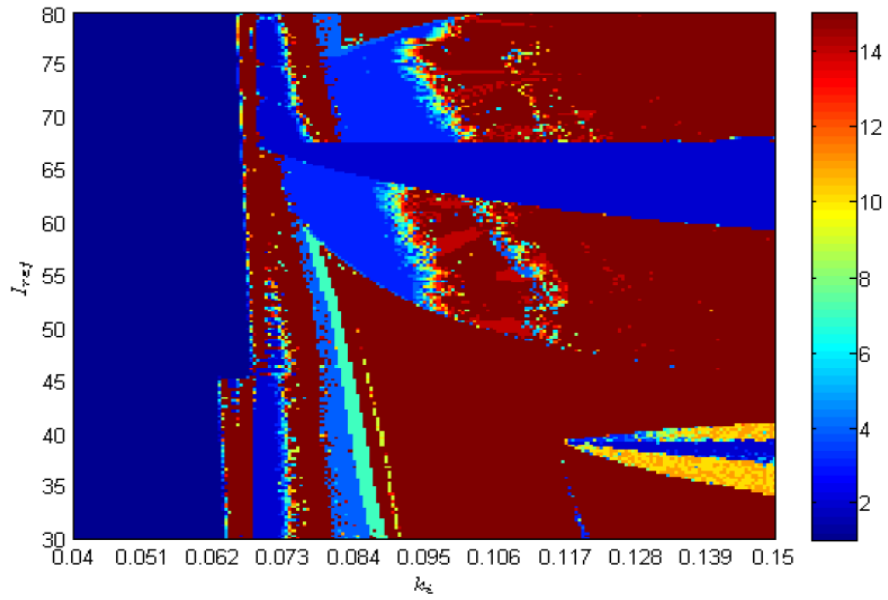

Figure 6-10: Periodicity diagram for duty cycle 1

For k_i marginally greater than 0.75, instead of converging to a single number, the duty cycle for switch one settles down to two values, there is no interspersion. This behavior continues as k_i is increased until 0.091, one period subharmonic emerges instead of two. Even though, there is a little range when $I_{ref} \approx 66A$; for the first k_i values, one subharmonic is registered. Later on, for a narrow range there is chaotic behavior and then it goes back to one subharmonic.

Figure **6-10** shows that the duty cycle for switch one is very dynamic. There are a lot of period n behavior in the right side of the figure, chaos is the most common one but there are some little domains where there are periodic domains. When $I_{ref} \approx 38A$, the behavior for the duty cycles starts with stability and finishes also stable. In the middle of both extremes, there are a lot of n-periodic and even chaotic ranges.

Figure **6-11** shows the last 50 values for each duty cycle in switch 1, for parameters k_i and I_{ref} combinations. It is easy to see that for the lowest values of the parameter k_i, there are fixed points, but this stability in the behavior ends after $k_i \approx 46A$. At this point, it is where the duty cycle values start to change because the control tries that the circuit variables reach the reference value. Even though as seen in figure **6-10**, sometimes this is achieved, some others it is not. It depends on the parameters values.

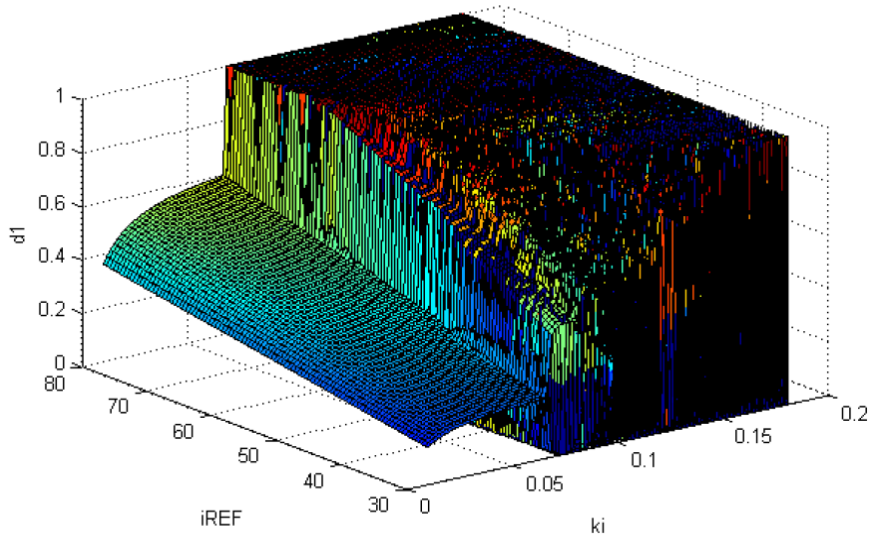

Figure 6-11: 2 parameter bifurcation diagram for duty cycle 1

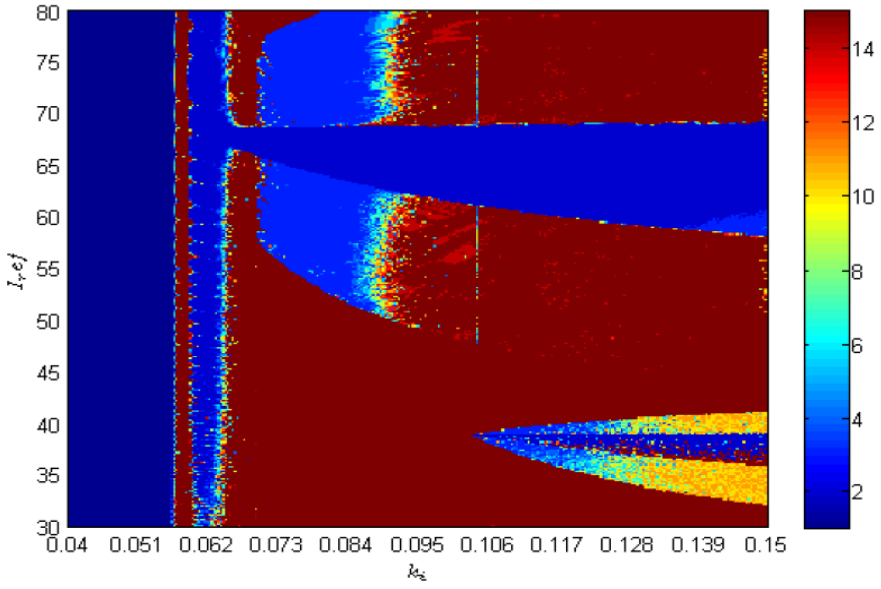

Figure 6-12: 2 parameter bifurcation diagram for duty cycle 1

Poincaré map approximation

In the fig. **6-12**, there is a diagram which describes the duty cycle for switch 1 diagram using the approximation for the matrix exponential in equation (3-37). When using both expressions, full

poincaré map and poincaré map with exponential matrix approximation, the duty cycle behavior is similar. As mentioned before for the system variables, some of the phenomenon or behavior, such as one periodic zones which are remarkable, appear for lower values of I_{ref}. This is expected, if the variables are affected this way, the most logical thing is that it affects the same way the switches duty cycles.

6.5 Duty cycle for switch 2

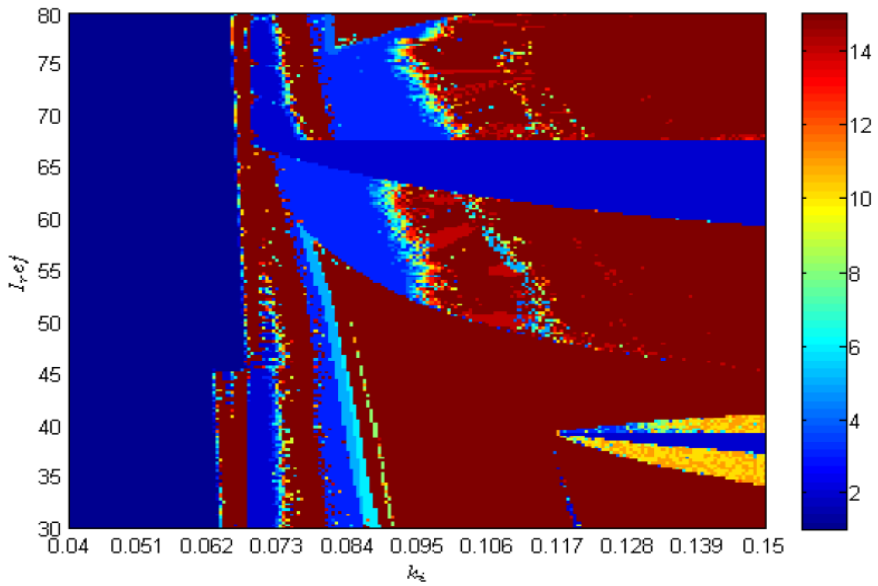

Figure 6-13: Periodicity diagram for duty cycle 2

Figure **6-13** shows the two parameters map for capacitor 2 voltage. In the left side of the figure, it is possible to recognize the stable domain which is suddenly interrupted by chaos, which lasts only for a very narrow range up to $k_i \approx 0.078$. For the lower I_{ref} values, there are two chaotic ranges separated by a stable one. Once the chaotic behavior finishes, there is a period 2 behavior for almost all the I_{ref} values except the ones around 68 A, which register stable behavior from $k_i \approx 0.078$ until $k_i \approx 0.18$. For I_{ref} values between 55 A and 80 A, after the period two behavior, the periodicity starts increasing and a pattern with cycles of length 2^n starts to be noticed.

Later on, for some cases as k_i increases, chaos and n- periodic behavior alternate, but at the end, chaos is the behavior that remains. Even though, when k_i starts getting closer to 0.163, periodic behavior starts appearing, and for values of I_{ref} between 68 A and 75 A, the behavior starts to converge to period 10, 11 and 12. For I_{ref} between 53 A and 60 A, the pattern of 2^n periods start

again and starts converging gradually to $2^{\inf}$, that is when chaos appear.

For I_{ref} values between 32 A and 42 A, and k_i between 0.12 and 0.18, there is a stable domain. For values near 37 A, and for values near the 32A and 42 A, the periodicity increases being 10, 11 and 12 the most common number of subharmonics registered in that area.

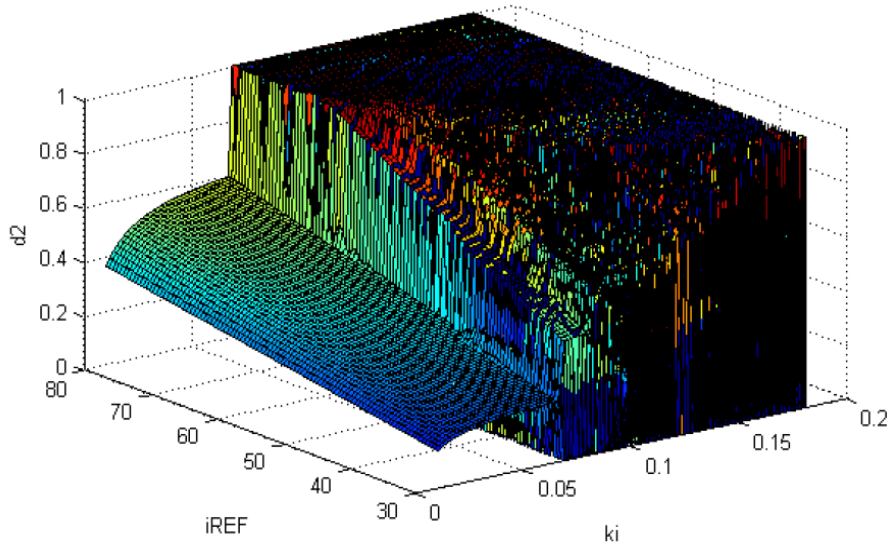

Figure 6-14: 2 parameter bifurcation diagram for duty cycle 2

Figure **6-14** looks alike figure **6-11**, there is a stable zone before $k_i \approx 0.68$ and once it takes this value, for the lowest values of the reference current I_{ref}, the periods start increasing and this is evidenced because it is possible to see how the values changes for d_1, this values are limited by saturation function and they can only be 0 or 1. As k_i increases, the duty cycles start varying more and more because they try to control the output variables, this sometimes is not possible to achieve.

Poincaré map approximation

For this fig.**6-15**, it is possible to see that when compared to fig.**6-13**, which is a 2 parameter bifurcation diagram, the periodicity is similar for both. As seen in the other approximation figures, the stable behavior appears for lower I_{ref} values, but in addition to this, the ten-periodic zone in the upper area remains.

A difference is that for the approximated model, in the 2 parameter map it is possible to see a new stable zone which is not present in fig.**6-13**, positioned for the high values of both I_{ref} and k_i.

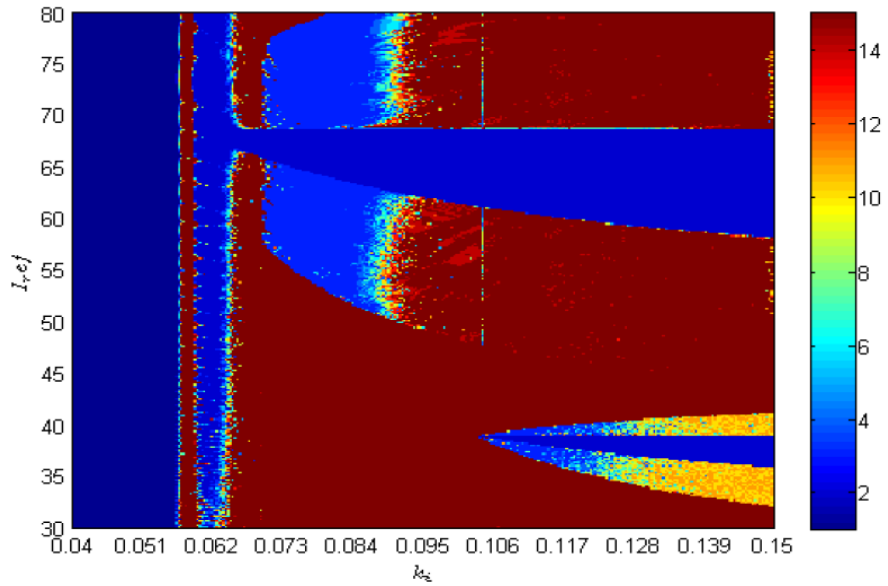

Figure 6-15: 2 parameter bifurcation diagram for duty cycle 2

6.6 Duty cycle for switch 3

All the switches duty cycles look alike, they have stable behavior in the same zone and the duty cycles values are almost the same for most of the parameter combinations. Even though, there are some parts where the periodicity changes and this is because each duty cycle depends on the values of the respective switch control signal. Figure **6-17** can be seen the evolution of the duty cycle in switch 3 for the different parameter combinations.In figure **6-16**, the periodicity for the duty cycle 3 for each parameter combination is shown.

For I_{ref} values between 30 A and 60 A, intermittentcy between stable, chaos and two periods is very common. For some cases six, ten and eleven period behavior is registered; there are other small parameter combination where the duty cycle value try to stabilize but for a narrow range of k_i because it later goes back to chaos but once k_i.

Poincaré map approximation

In the duty cycle of switch 3, happens the same as mentioned for the approximated poincaré map, there is a new stable zone that was no visible in the figure obtained without approximation and also, the phenomena happen in a similar way but for the whole poincaré map expression, it takes

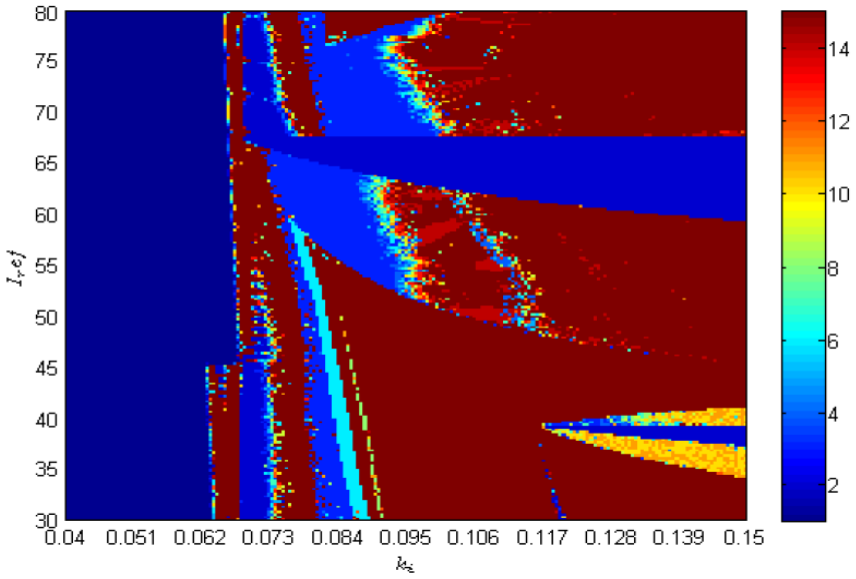

Figure 6-16: Periodicity diagram for duty cycle 3

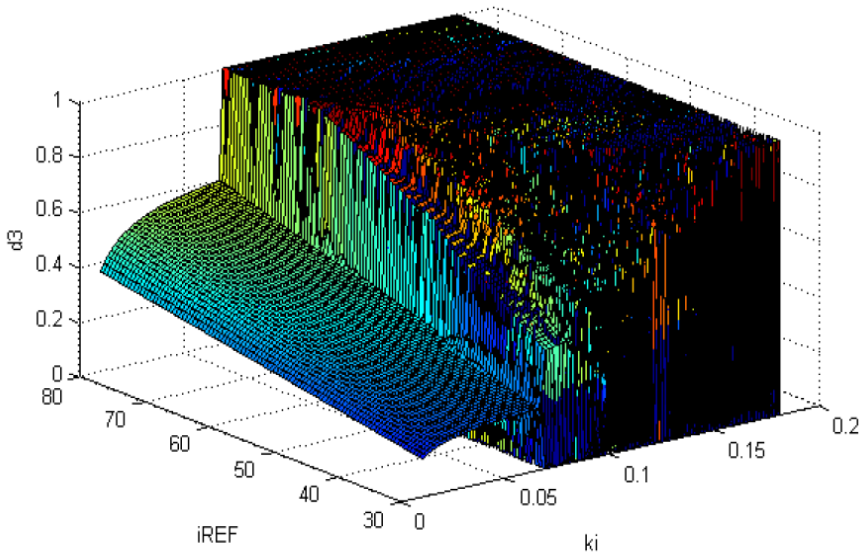

Figure 6-17: 2 parameter bifurcation diagram for duty cycle 3

place in higher values of I_{ref}.

This is expected because the control makes the three control signals to be the same or at least, as similar as possible.

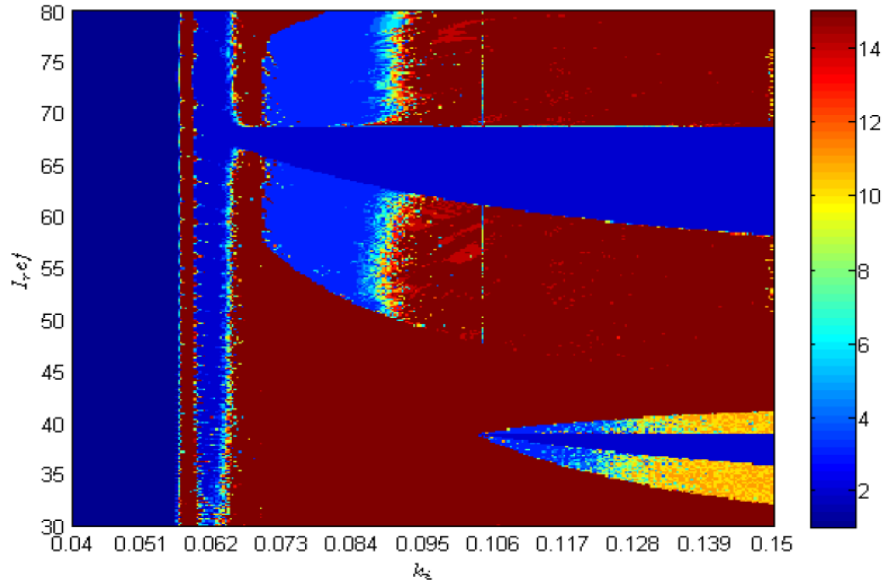

Figure 6-18: 2 parameter bifurcation diagram for duty cycle 3

7 Conclusions

- The three-cell buck converter controlled with digital PWM mathematical analysis was done using mathematical simulation and discrete time modeling. The results obtained with the developed mathematical algorithm were compared with simulation software results, the results obtained with the algorithm are similar.
- The discrete time modeling is a very efficient method, it is possible to obtain results in less time than any other method takes; it is also very accurate and the advantage of using Poincaré maps is that stability study can be done.
- The approximation used for the Poincaré map method improves the computational time of response and graphics are obtained in less time. Eventhough, the one and two dimensional bifurcation diagrams for the voltages in capacitors are not similar to the ones obtained with the normal Poincaré map method. This technique has been used to analyze other circuits with successful results. There is a possibility that to decrease the computational time, this approximation may not be the best idea and other methods can be explored.
- The Poincaré map discrete time modeling was successfully implemented, fixed points were obtained through an algorithm designed to do the mathematical procedure and results were compared to the graphics obtained with the algorithm to describe the system and also with simulation in PSIM software.
- The effect of the circuit parameters, which are as well the control signal constants, was analyzed by obtaining variable response graphics for bigger and smaller magnitudes for the load, inductor and capacitors and by obtaining and analyzing bifurcation diagrams.
- The two and three dimensional bifurcation diagrams were obtained, they allowed to understand better the effect of the parameters k_i and I_{ref} in the system variables and duty cycles. These parameters are analyzed in detail due to the use od the current to obtain the output voltage in the load.
- A range of values for the parameters k_i and I_{ref} can be obtained from the diagrams that describe the current in the inductor and voltages in the capacitors present in the three-cell buck converter in order to make sure the system has a stable behavior.
- The method to analyze the stability of the periodic orbits was successfully implemented, the first bifurcation can be detected for the approximated poincaré map expression.

Future work

Experimental validation is a subject of future study, physical proves could be done and the circuit can be properly tested. Extension of the results using other control methods or other multi-cell converters are considered and would contribute to the field of study.

The three cell buck converter behavior can be analyzed using many different methods. This thesis has results obtained with the Poincaré map method. Other methods can be implemented as well and compared with the ones in this thesis and with simulations.

Bibliography

[1] D. C. Hamill and D. J. Jefferies. Subharmonics and chaos in a controlled switched-mode power converter. *IEEE Transactions on Circuit and Systems-I*, 35:1059–1061, 1988.

[2] J. H. B. Deane and D. C. Hamill. Instability, subharmonics and chaos in power electronic systems. *IEEE Transactions on Power Electronics*, 5(3):260–268, 1990.

[3] E. Van Dijik, J. N. Sprujit, and D. M. O'Sullivan. Pwm switch modeling of dc-dc converters. *IEEE Transactions on Power Electronics*, 10, No.(6):659–665, 1995.

[4] K. Chakrabarty, G. Poddar, and S. Banerjee. Bifurcation behavior of the buck converter. *IEEE Transactions on Power Electronics*, Vol 11. No 3:439–447, 1996.

[5] E. Fossas and G. Olivar. Study of chaos in the buck converter. *IEEE Transactions on Circuits and Systems*, Vol. 43, No. 1:13–25, 1996.

[6] W. C. Y. Chan and C. K. Tse. Study of bifurcations in current programmed dc-dc boost converters: from quasiperiodicity to period-doubling. *IEEE Transactions on Circuits and Systems*, Vol. 44, No. 12:1129–1142, 1997.

[7] Z. Galias. Exploiting the concept of conditional, transversal lyapunov exponents for study of synchronization of chaotic circuits. In *Circuits and Systems, 1998. ISCAS '98. Proceedings of the 1998 IEEE International Symposium on*, volume Vol. 4, 31, pages 568–571, 1998.

[8] M. Di Bernardo, F. Garofalo, L. Glielmo, and F. Vasca. Switchings, bifurcations, and chaos in dc-dc converters. *IEEE Transactions on Circuits and Systems*, Vol. 45, No. 2:133–141, 1998.

[9] M. Di Bernardo, C. Budd, and A. Champneys. Grazing, skipping and sliding: analysis of the non-smooth dynamics of the dc-dc buck converter. *Nonlinearity*, Vol. 11:858–890, 1998.

[10] G. Yuan and S. Banerjee. Border collisions bifurcation in the buck converter. *IEEE Transactions on Circuits and Systems*, Vol. 45, No. 7:707–716, 1998.

[11] G. Olivar, E. Fossas, and C. Batle. Bifurcations and chaos in converters: Discontinuous vector fields ans singular poincaré maps. *Nonlinearity*, Vol. 13:1095–1121, 2000.

[12] I. Fleggar, D. Pelin, and D. Zacek. Bifurcation diagrams of the buck converter. *9th International conference on Electronics, Circuits and Systems*, Vol. 3:975–978, 2002.

[13] R. Ramos, D. Biel, E. Fossas, and Guin. A fixed-frequency quasi-sliding control algorithm: Application to power inverters design by means of fpga implementation. *IEEE Transactions on Power Electronics*, Vol. 18, No. 1, 2003.

[14] F. Angulo. *Dynamical Analysis of PWM-controlled power electronic converters based on the zero average dynamics (ZAD) strategy*. PhD thesis, Technical University of Catalonia, 2004.

[15] Yu. A. Kuznetsov, S. Rinaldi, and A. Gragnani. One-parameter bifurcations in planar filippov systems. *International Journal of Bifurcation and Chaos*, Vol. 13, No. 8:2157–2188, 2003.

[16] A. El Aroudi, B. Robert, and L. Martinez-Salamero. Bifurcation behavior of a three cell dc-dc buck converter. *EPE-PMEC*, pages 1994–2001, 2006.

[17] G. Gateau, P. Maussion, and T. Meynard. De la modélisation à la commande non linéaire des convertisseurs multicellulaires série. application à la fonction hacheur. *J. Phys III France 7*, pages 1277–1305, 1997.

[18] B. Robert and A. El Aroudi. Discrete time model of a multi-cell dc/dc converter: Non linear approach. *Mathematics and Computers in Simulation*, 71:310–319, June 2006.

[19] A. El Aroudi and B. Robert. Stability analysis of a voltage mode controlled two-cells dc-dc buck converter. *Power Electronics Specialists Conference*, pages 1057 – 1061, 2005.

[20] A. El Aroudi, F. Angulo, B. Robert, M Feki, and G. Olivar. Widening stability zone of a multi-cell dc-dc buck converter by using fixed point induced control. *Power System Conference, 2008. MEPCON 2008. 12th International Middle-East*, pages 583 – 587, 2008.

[21] A. El Aroudi, F. Angulo, G. Olivar, B.G.M. Robert, and M Feki. Stabilizing a two-cell dc-dc buck converter by fixed point induced control. *International Journal of Bifurcation and Chaos*, 19(6):2043–2057, 2009.

[22] D. Patino, M. Bâja, H. Commerais, P. Riedinger, J. Buisson, and C. Iung. Alternative control methods for dc-dc converters. an application to a four-level three-cell dc-dc converter. *International Journal of Robust and Nonlinear Control 21*, 2011.

[23] M. J. Feigenbaum. Universal behavior in nonlinear systems. *Los Alamos Science*, Vol. 1:4–27, 1980.

[24] D. J. Jefferies, J. H. B. Deane, and G. G. Johnstone. An introduction to chaos. *Electron. and comm. Engg. J.*, Vol. 1, No. 3:115–123, 1989.

[25] T. A. Meynard, M. Fadel, and N. Aouda. Modeling of multilevel converters. *IEEE Transactions on industrial electronics*, 44:356–364, 1997.

[26] K. Kaoubaa, J. Pelaez-Restrepo, M. Feki, B. G. M. Robert, and A. El Aroudi. Improved static and dynamic performances of a two-cell dc-dc buck converter using a digital dynamic time-delayed control. *International Journal of Circuit Theory and Applications*, 2009. Avaliable online at http://dx.doi.org/10.1002/cta.735.

[27] A. El Aroudi, M. Debbat, and L. Martinez-Salamero. Poincaré maps modeling and local orbital stability analysis of discontinuous piecewise affine periodically driven systems. *Nonlinear Dynamics*, 50:431–445, 2007. 10.1007/s11071-006-9190-1.

[28] A. El Aroudi, B.G.M. Robert, A. Cid-Pastor, and L. Martinez-Salamero. Modeling and design rules of a two-cell buck converter under a digital PWM controller. *Power Electronics, IEEE Transactions on*, 23(2):859–870, March 2008.

[29] B. Robert and A. El Aroudi. Discrete time model of a multi-cell dc/dc converter: Non linear approach. *Mathematics and Computers in Simulation*, 71:310–319, 2006.

[30] S. H. Strogatz. *Non linear dyanmics and chaos*. Perseus Book Publishing, 1994.